



Progress and Prospects of X-ray Free Electron Lasers

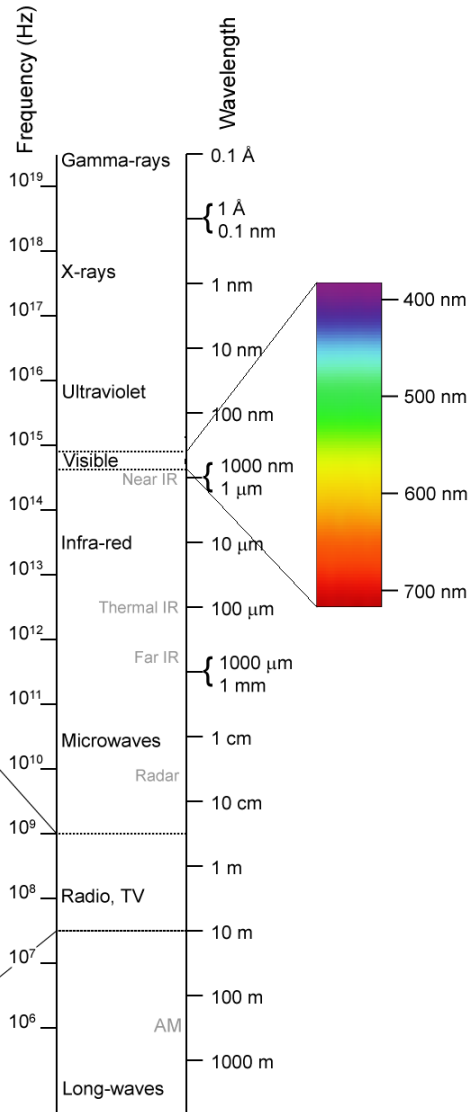
Evgeny Saldin

The dream of an X-ray laser has motivated the laser community for many decades, but quantum lasers can only be operated to EUV range.

The history of coherent source for X-ray range began in 1977 with the conception of the Free Electron Laser by John Madey.

Today, XFELs are capable of operation over entire X-ray spectrum and of producing femtosecond fully coherent pulses with peak power up to 100 GW-level

X-ray FELs have become part of the vocabulary of mankind



XFELs

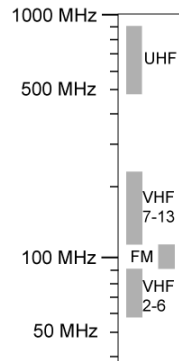
early 21th century

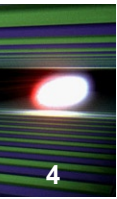
Quantum lasers

Vacuum tube devices

early 20th century

Electromagnetic
Spectrum



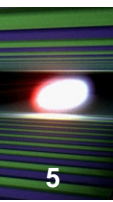


X-ray FEL is the central subject to this talk, to be outlined in three separate parts as follows:

(I) FEL theory results

(II) Inventions

(III) Applications



A. Kondratenko and E. Saldin Part. Accel. 10, 207 (1980)

In this paper, for the first time the possibility was considered of using high gain regime of amplification, starting from spontaneous emission, to reach saturation in the single pass infrared FEL.

This paper opened up the possibility of using the same approach at shorter wavelengths and extend FEL to the X-ray region.

Particle Accelerators
1980 Vol.10 pp.207-216
0031-2460/80/1003-0207\$06.50/0

© Gordon and Breach, Science Publishers, Inc.
Printed in the United States of America

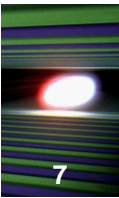
GENERATION OF COHERENT RADIATION BY A RELATIVISTIC ELECTRON BEAM IN AN ONDULATOR*

A. M. KONDRATENKO and E. L. SALDIN

Institute of Nuclear Physics, 630090, Novosibirsk, USSR

(Received January 28, 1980)

* See also Preprint INP 79-48, Novosibirsk, 1979.

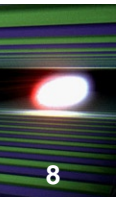


5. ON THE LEVEL OF BEAM MODULATION AT THE ENTRANCE OF AN ONDULATOR

To reveal the effect of self-modulation, a knowledge of the initial level of the harmonics of beam density is necessary. In a realistic situation, if the initial conditions are not prepared in a special manner, there exists a continuous spectrum of fluctuations of density harmonics that arise from the fact that there is a finite number of particles in the beam. Hence all the harmonics in a band of width $(\Delta K/K) \approx \kappa_0/l$ will become unstable and grow by a few times in the length l . After passage of a length $L \approx l \cdot \ln(\rho_0/\bar{\rho}_i)$ all the harmonics achieve a size of the order of ρ_0 .

The spectrum width $\Delta K \sim K\kappa_0/l$ corresponds to a correlation length of the order of $l/2\gamma_{\parallel}^2$. Hence the values of harmonics of density fluctuations for the narrow and wide beams respectively are

$$\begin{aligned} \bar{\rho}_i/\rho_0 &\approx (Nl/2\gamma_{\parallel}^2)^{-1/2}, \quad \bar{\rho}_i/\rho_0 \\ &\approx (Nl/2\gamma_{\parallel}^2)^{-1/2}(\sigma^2/\kappa l)^{1/2}. \end{aligned}$$



Ya. Derbenev, A. Kondratenko and E. Saldin Nucl. Instrum. and Methods 193 (1982)

In this paper, for the first time the possibility was considered of using high gain FEL amplifier starting from noise, inserted in storage ring, to produce soft X-rays

Nuclear Instruments and Methods 193 (1982) 415–421
North-Holland Publishing Company

ON THE POSSIBILITY OF USING A FREE ELECTRON LASER FOR POLARIZATION OF ELECTRONS IN STORAGE RINGS

Ya.S. DERBENEV, A.M. KONDRATENKO and E.L. SALDIN

Institute of Nuclear Physics, 630090, Novosibirsk 90, U.S.S.R.

Received 20 October 1980 and in revised form 17 August 1981

The possibility to polarize electrons (or positrons) by colliding with circularly polarized photons is discussed. For this purpose the coherent radiation of relativistic electron beams in the helical undulator is proposed. The possibility of polarizing by soft photons without beam loss in the storage ring is demonstrated. The cyclic version of the hard coherent radiation source (i.e. an X-ray laser) is proposed for polarization by the knock-out method. It has been shown that the use of a free electron laser enables the construction of an intense polarized positron beam source.

The density modulation increment is determined by the peak current $e\dot{N}$ in the FEL beam, its transverse area $2\pi\sigma^2$, the value of the transverse rotation velocity u driven by the undulator and by the energy of an electron source $\epsilon_s = \gamma_s mc^2$. For a wide beam, when

$$\sigma^2 \gg \sigma_0^2 = \frac{\lambda_{\text{ph}}^2}{u} \left[\frac{\gamma_s \gamma_{11}^2 c^3}{\dot{N} r_e} \right]^{1/2},$$

($r_e = e^2/mc^2$) the growth length is minimum at the exact resonance (3) and is equal to [5–11]:

$$l_g = \frac{2^{4/3}}{3^{1/2}} \frac{1}{\lambda_{\text{ph}}} (\sigma^2 \sigma_0^4)^{1/3}. \quad (4)$$

In the case of a narrow beam ($\sigma^2 \ll \sigma_0^2$), the growth length is approximately equal to [10,11]:

$$l_g \simeq \frac{\sigma_0^2}{\lambda_{\text{ph}}} \left[\ln \frac{\sigma_0}{\sigma} \right]^{-1/2} \quad (5)$$

The beam, after its passage through the length $L = l_g \cdot \ln 1/a$, where (a) is the degree of initial beam modulation on the resonant harmonic, will have a modulation degree of the order of unity, and in this state it will radiate over a length of the order of l_g . The coherent radiation power W will have an order of

magnitude,

$$W \simeq \dot{N} \epsilon_s \lambda_0 / l_g. \quad (6)$$

The statistical fluctuations of beam density, which are caused by the finite number of particles, will play the role of an initial excitation of modulation. For example, for a narrow beam

$$a_{\text{fl}} \approx [2\gamma_{11}^2 c / \dot{N} l_g]^{1/2}.$$

In the development of the modulation from the spectrum of density fluctuations the angular divergence of the output radiation is approximately equal to ($\gamma_{11} \theta_{\text{ph}} \ll 1$)

$$\theta_{\text{ph}} \approx (\lambda_{\text{ph}} / l_g)^{1/2}, \quad \sigma^2 \ll \sigma_0^2$$

$$\theta_{\text{ph}} \approx \max \left[\frac{\sigma}{L}, (\lambda_{\text{ph}} / l_g)^{1/2} \right], \quad \sigma^2 \gg \sigma_0^2.$$

Radiation instability occurs if the particle shifts due to the spread of longitudinal velocities may be ingored over length of the order of l_g :

$$(\Delta\beta_{11} l_g)^2 \ll \lambda_{\text{ph}}^2.$$

The longitudinal velocity spread results from the energy and angular spreads:

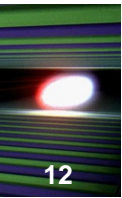
$$(\Delta\beta_{11})^2 = \frac{1}{\gamma_{11}^4} \left(\frac{\Delta\epsilon_s}{\epsilon_s} \right)^2 + \frac{1}{4} (\Delta\theta)^4.$$

consider an electron beam with the following parameters: $\gamma \simeq 4 \times 10^4$, the number of particles in the beam $N_e \simeq 10^{13}$, the bunch length $l_b \simeq 3$ cm, the horizontal beam emittance $\sigma_x \Delta\theta_x \simeq 5 \times 10^{-7}$ cm, the beam size $\sigma_z \simeq 0.1\sigma_x$. Let this beam pass through an helical undulator with period $\lambda_0 = 7$ cm and magnetic field $H_0 = 20$ kG. In this case, the resonant wavelength of the coherent radiation is equal to $\lambda = (2\gamma_{11}^2)^{-1} \lambda_0 = 5 \times 10^{-7}$ cm. The characteristic growth length of the density modulation, with the transverse size in the undulator; $\sigma_x \sigma_z \simeq 10^{-5}$ cm², is calculated by eq. (4) and is equal to $l_g \simeq 200$ cm. To perform the beam self-modulation it is necessary that the angular and energy spreads should satisfy the conditions

$$(\Delta\theta)^2 \lesssim 10^{-9}, \quad \Delta\gamma/\gamma \lesssim 0.5 \times 10^{-2}.$$

In conclusion, we would like to mention that storage ring-generators are, in essence, X-ray lasers. In our opinion, the creation of such devices is within the scope of present-day acceleration technology.

For a given phase space volume of the circulating beams, these conditions may be fulfilled if the value of the β -function in the undulator is of the order of 5 m. The required length of the undulator in the development of modulation from the spectrum of fluctuations is of the order of 15 m. The fraction of the beam energy converted into coherent radiation during one flight will amount to about 0.5%. The area of the radiated beam at its exit from the undulator is of the order of that of the circulating electron beam in the undulator and the radiated beam divergence angle is $\simeq 3 \times 10^{-5}$. The peak radiation power (on a wavelength of 5×10^{-7} cm and with the degree of monochromaticity $\Delta\lambda/\lambda \simeq 10^{-2}$) is approximately 10^{12} W.



	XFEL (1982)	EXFEL(SASE3)
Electron energy	20 GeV	10-17.5 GeV
Undulator period	7 cm	7 cm
Photon energy	0.25 keV	0.25 -3 keV
Peak current	14 kA	5-10 kA
Field gain length	~ 2 m	~ 2 m *
Output peak power	~ 1 TW	~ 1 TW **

Review of x-ray free-electron laser theory

Zhirong Huang

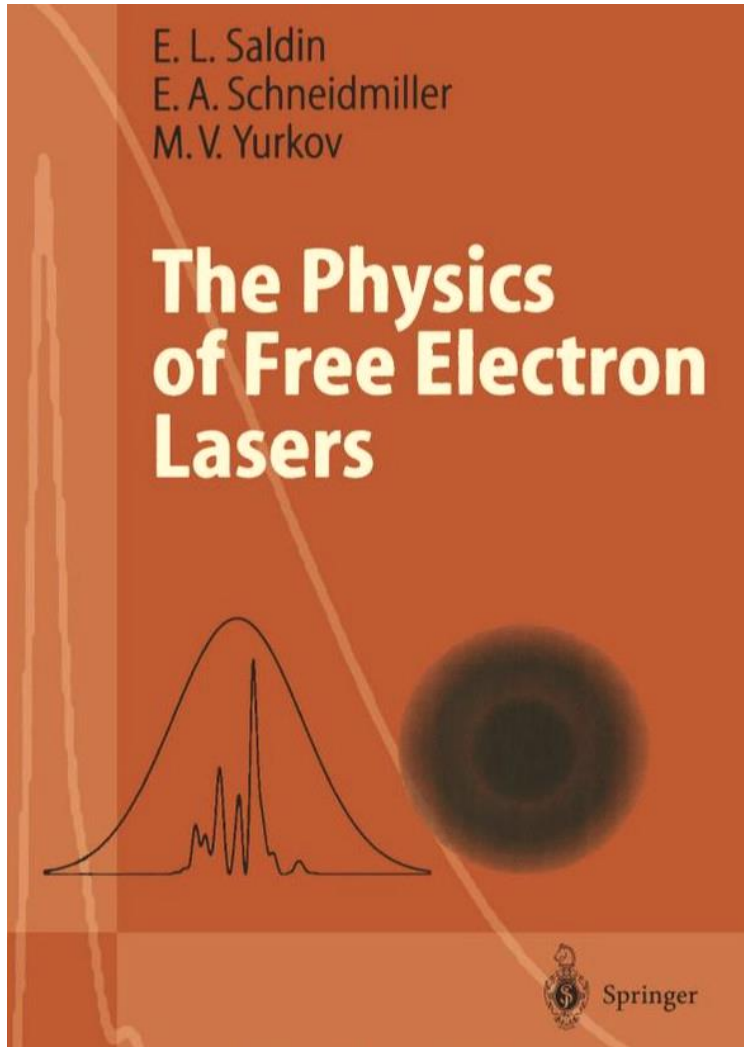
Stanford Linear Accelerator Center, Stanford, California 94309, USA

Kwang-Je Kim

Argonne National Laboratory, Argonne, Illinois 60439, USA

(Received 25 August 2006; published 12 March 2007)

- [1] J. Madey, *J. Appl. Phys.* **42**, 1906 (1971).
 - [2] D. A. G. Deacon, L. R. Elias, J. M. J. Madey, G. J. Ramian, H. A. Schwettman, and T. I. Smith, *Phys. Rev. Lett.* **38**, 892 (1977).
 - [3] A. Kondratenko and E. Saldin, *Part. Accel.* **10**, 207 (1980).
 - [4] Y. Derbenev, A. Kondratenko, and E. Saldin, *Nucl. Instrum. Methods Phys. Res., Sect. A* **193**, 415 (1982).
 - [5] R. Bonifacio, C. Pellegrini, and L. Narducci, *Opt. Commun.* **50**, 373 (1984).
-



The work of the period 1979 to 1999 is summarised in this monograph

- Series: Advanced Texts in Physics
- Paperback: 470 pages
- Publisher: Springer; Softcover reprint of hardcover 1st ed. 2000 edition
- Language: English
- ISBN-10: 3642085555
- ISBN-13: 978-3642085550

DESY 15-021

Theoretical computation of the polarization characteristics of an X-ray Free-Electron Laser with planar undulator

Gianluca Geloni^a Vitali Kocharyan^b Evgeni Saldin^b

^a*European XFEL GmbH, Hamburg, Germany*

^b*Deutsches Elektronen-Synchrotron (DESY), Hamburg, Germany*

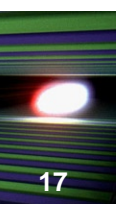
ISSN 0418-9833

Exact inhomogeneous wave equation for electric field

$$c^2 \nabla^2 \vec{E} - \frac{\partial^2 \vec{E}}{\partial t^2} = 4\pi c^2 \vec{\nabla} \rho + 4\pi \frac{\partial \vec{j}}{\partial t}$$

The current source provides the main contribution to the radiation field in an FEL amplifier and the contribution of charge term is negligibly small

$$W_\pi / W_\sigma \simeq 1.5 \cdot 10^{-7}$$

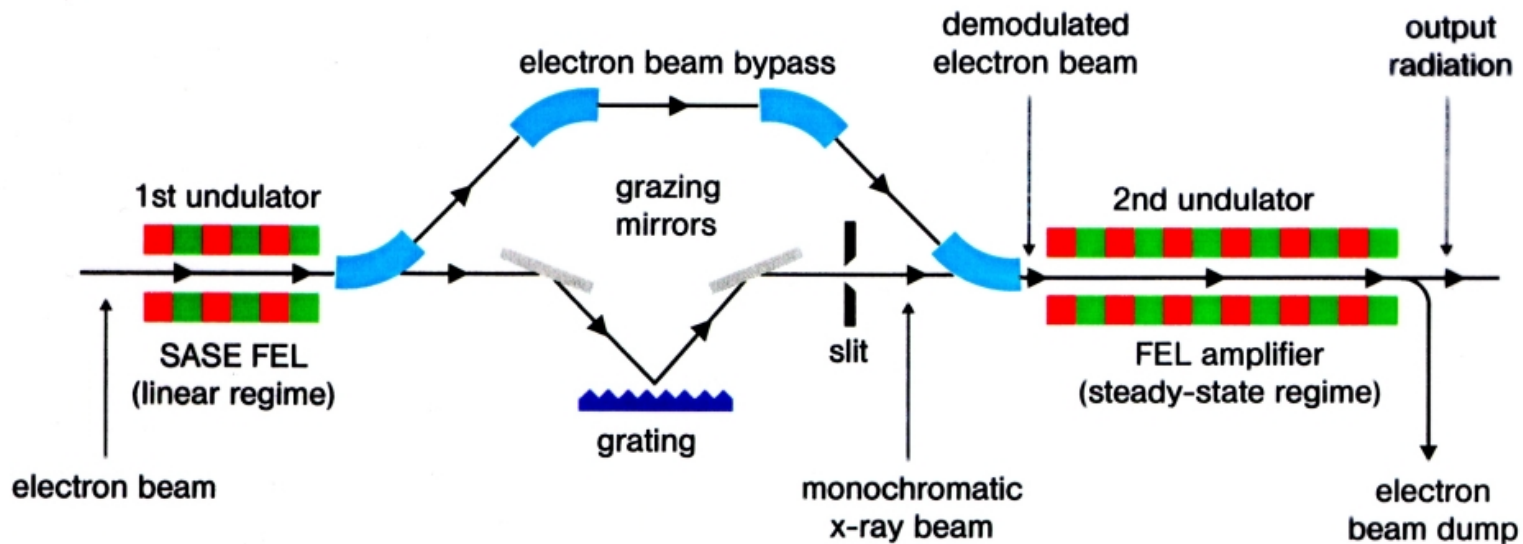


FEL literature is full of brilliant ideas that did not work...

...but self-seeding is an idea that does definitely work.

- Self-seeding opened a route to XFEL with laser-like output characteristics
 - Self-seeding works best from 5 nm down to 0.1 nm
-

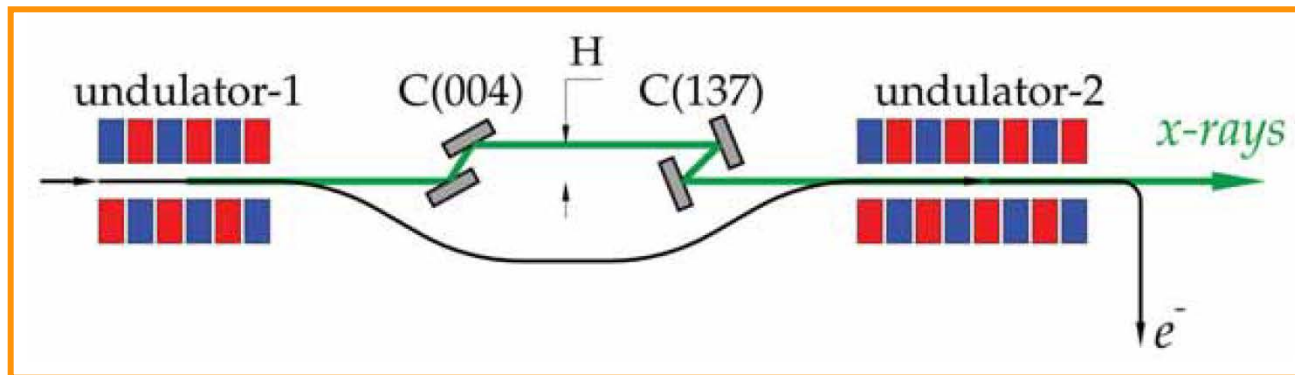
- First undulator generates SASE
- X-ray monochromator filters SASE and generates seed
- Chicane delays electrons and washes out SASE microbunching
- Second undulator amplifies seed to saturation

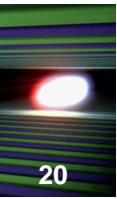


¹ J. Feldhaus, E.L. Saldin, J.R. Schneider, E.A. Schneidmiller, M.V. Yurkov, *Opt. Comm.*, V.140, p.341 (1997)

Grating monochromator substituted by crystal monochromator for applications to hard x-rays
[E. Saldin, E. Schneidmiller, Yu. Shvyd'ko and M. Yurkov, NIM A 475 357 (2001)]

Extra x-rays path due to monochromator ~ 1 cm. Long electron bypass (tens of meters) needed





Quite surprisingly, monochromatization can be performed by an almost trivial setup of as few as two components:

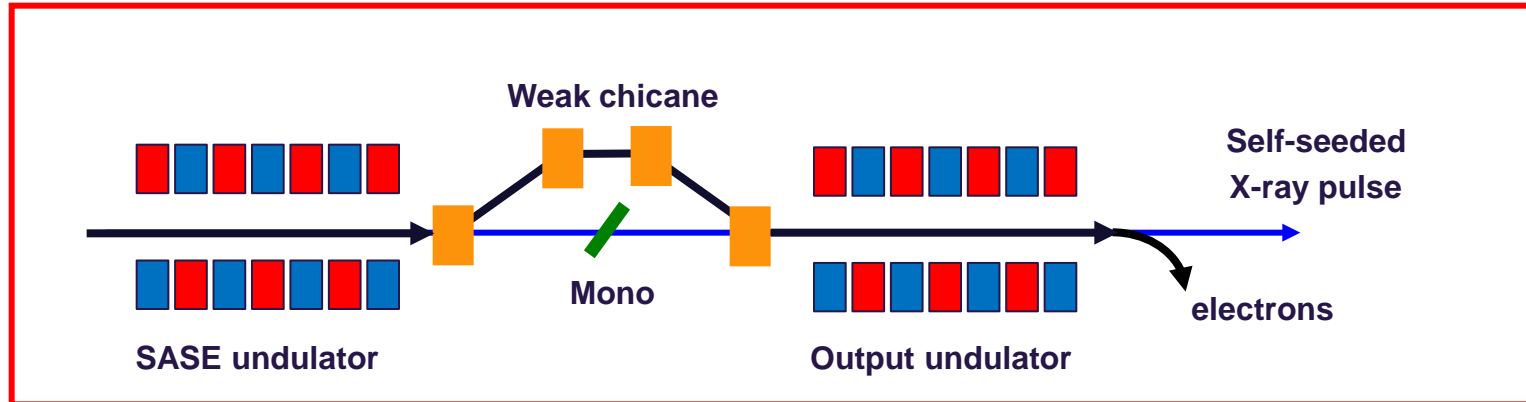
- a short (3 m-long) chicane and
- a single crystal



HXRSS scheme with single-crystal monochromator:

G. Geloni, V Kocharyan, E Saldin
J. Modern Opt. 2011; 58:1391-14303

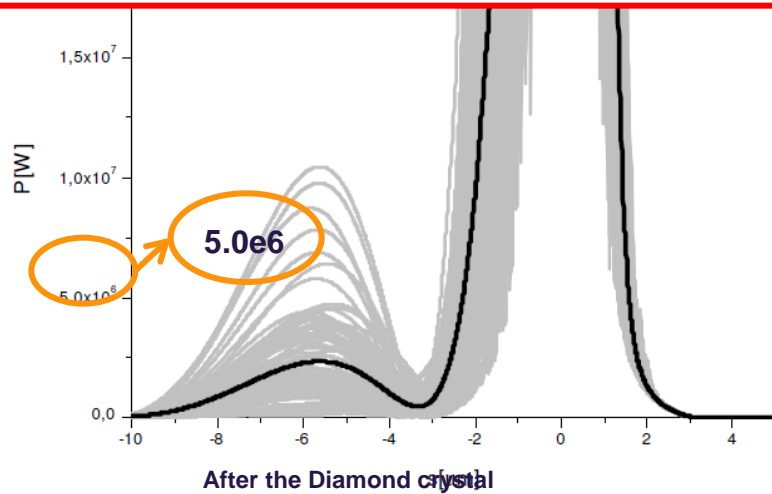
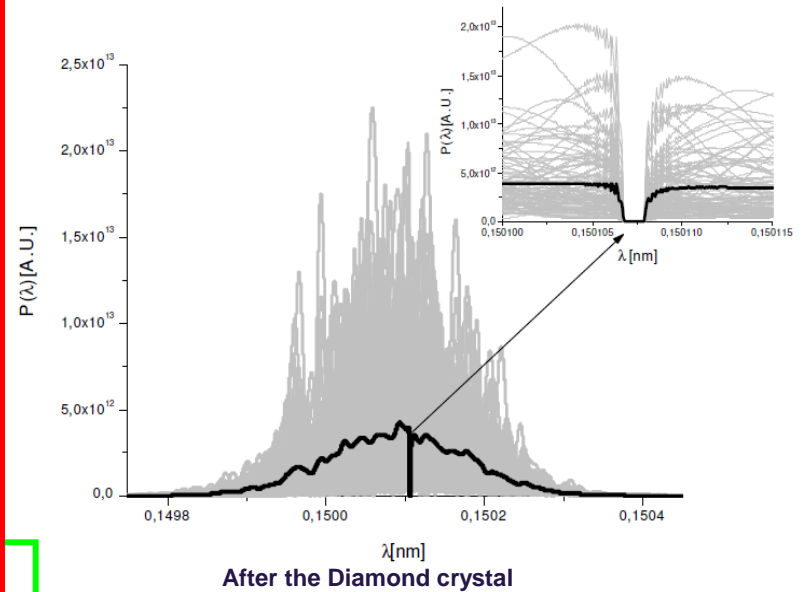
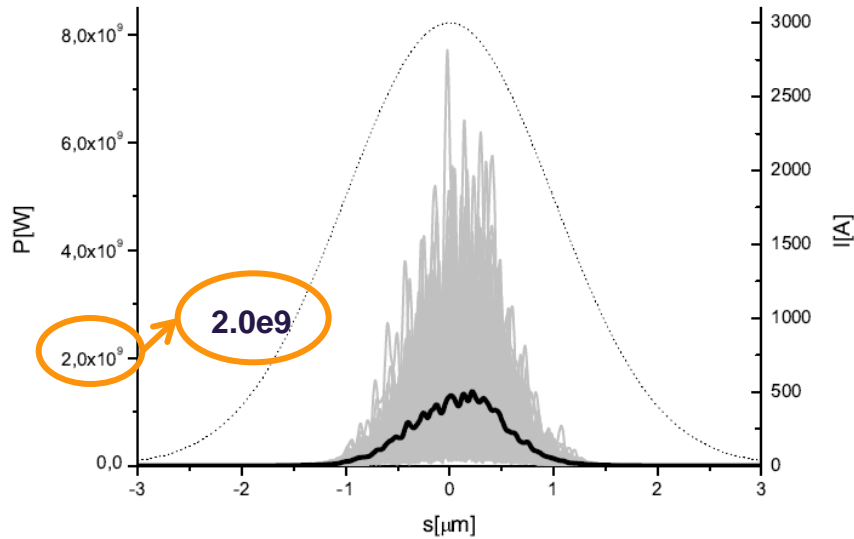
Working principle



Monochromatization of X-rays using a single crystal in Bragg-transmission geometry.

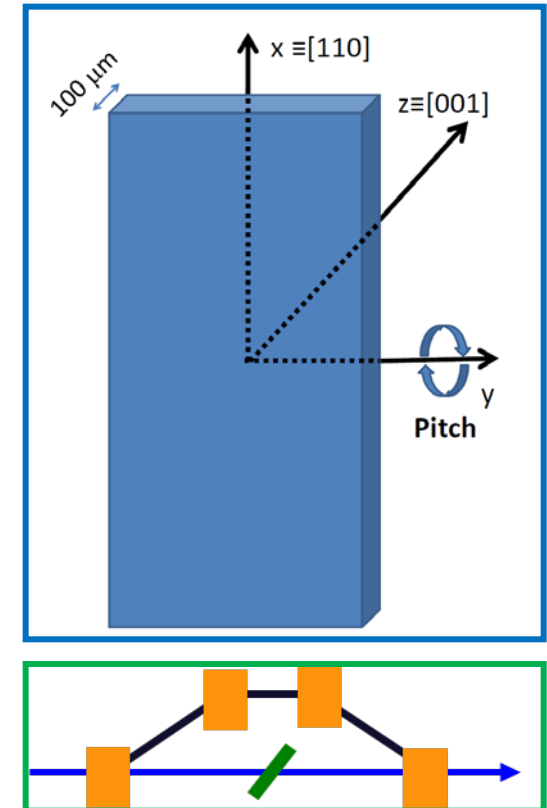
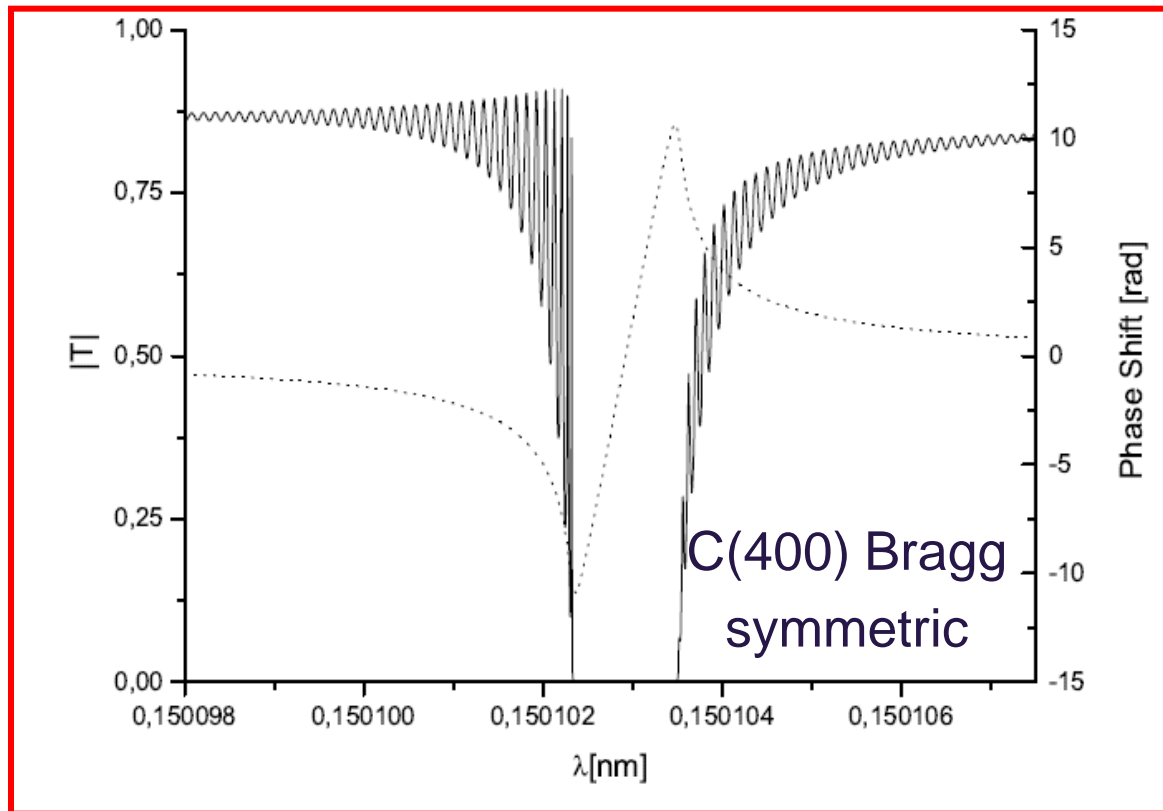
Monochromator introduces no path delay of X-rays, thus avoiding the need for a long electron beam bypass, as required in schemes with the monochromator in Bragg reflection geometry

The scheme is extremely compact and based on the substitution of a single undulator module with a weak chicane and single crystal



**Efficient seeding mechanism
(monochromatic tail
much larger than shot noise)
is achieved**

*G. Geloni, V. Kocharyan, E. Saldin
DESY 10-133*



The monochromator hardware is constituted by a single crystal. The forward diffracted beam is considered. In the space-frequency domain, the crystal acts as a band stop filter (modulus and phase).
Characterization of the filter needed.

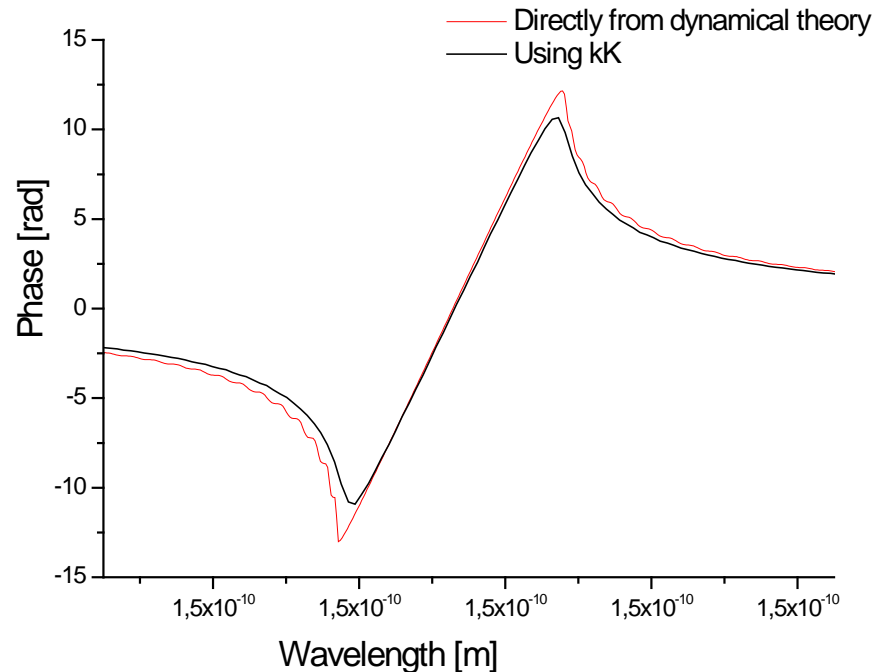
This can be shown, proving directly that

$$T = T(\eta)$$

Has no zeros on the upper complex plane (so that $\ln[|T|]$ is not singular and we can recover the phase).

So, knowing $|T|$ from e.g. XOP or other easily available programs, we use

$$\Phi(\omega) = -\frac{2\omega}{\pi} \mathcal{P} \int_0^{\infty} \frac{\ln[|T(\omega')|]}{\omega'^2 - \omega^2} d\omega'$$

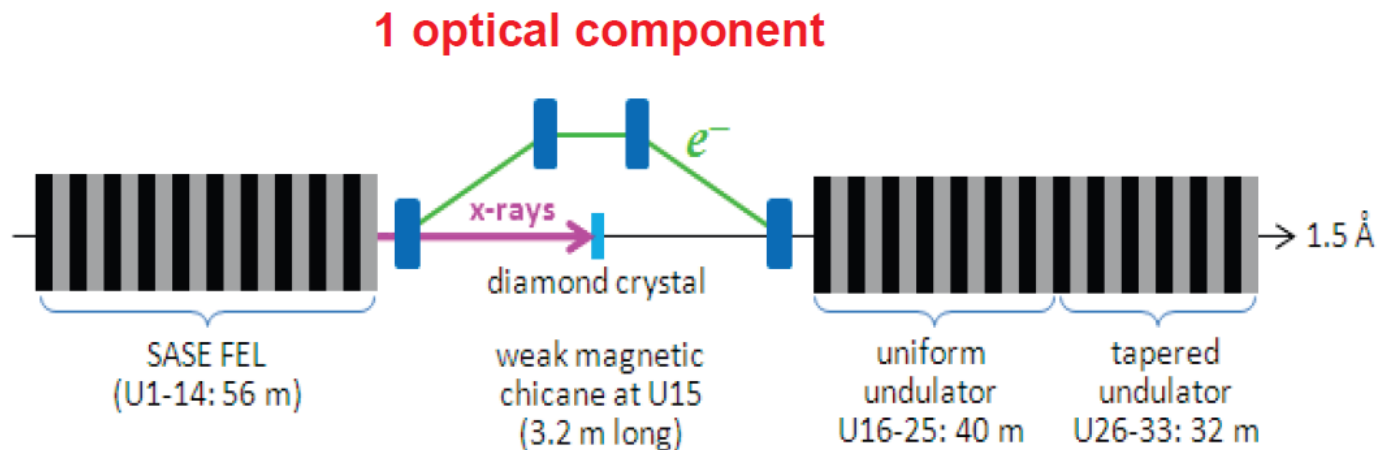


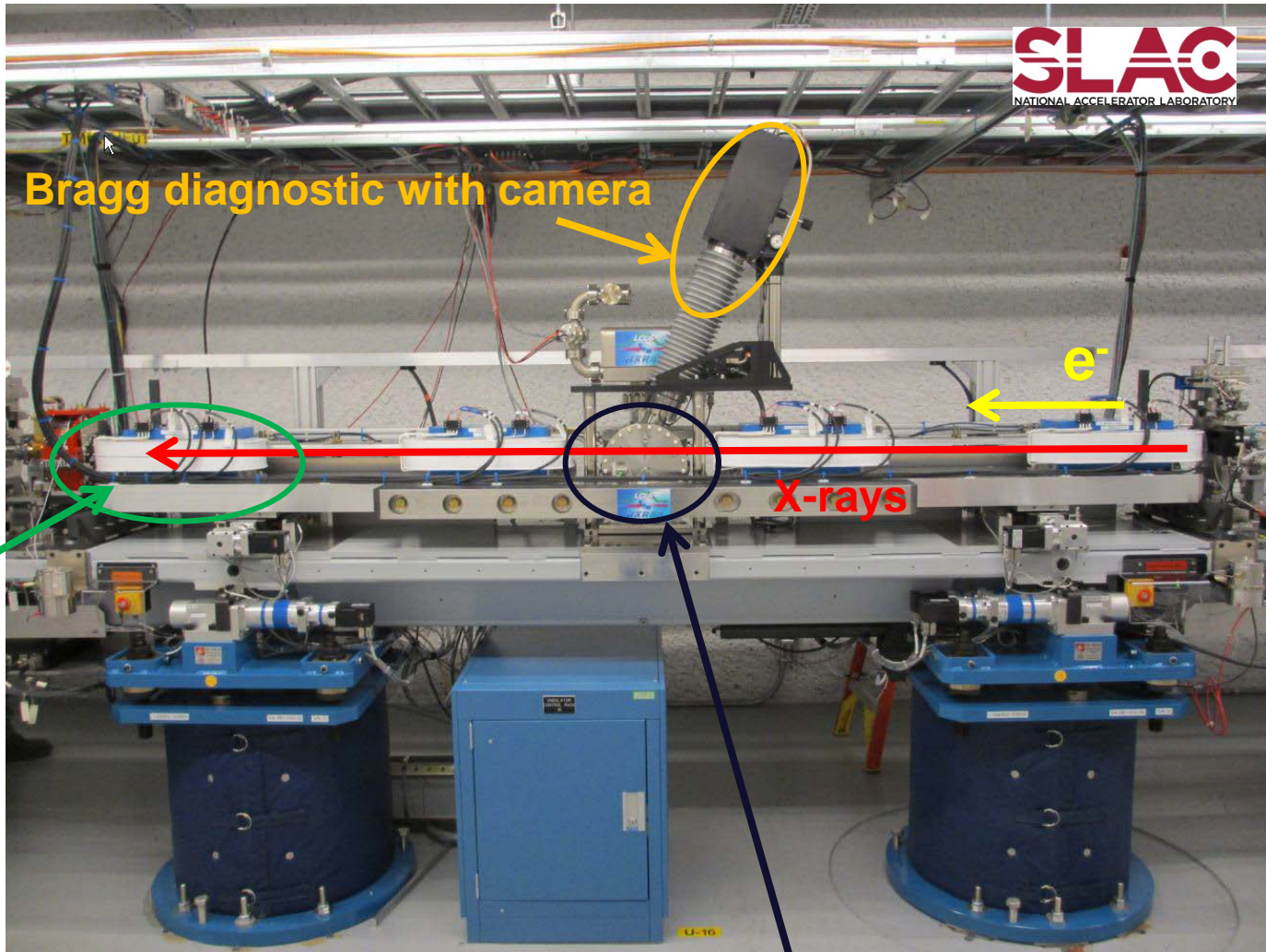


Demonstration of self-seeding in hard-X-ray free electron laser, Amman, et al.

Nature Photonics,
DOI:10.1038/NPHOTON 2012.180

HXRSS



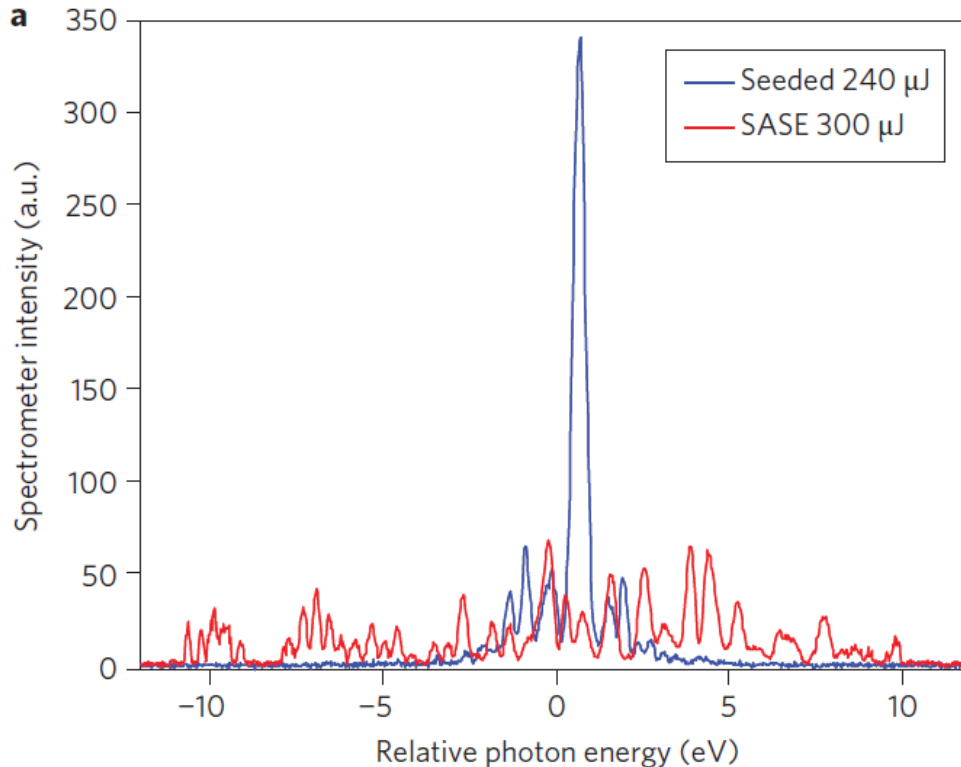


Chicane magnet

Bragg diagnostic with camera

X-rays

Diamond mono chamber

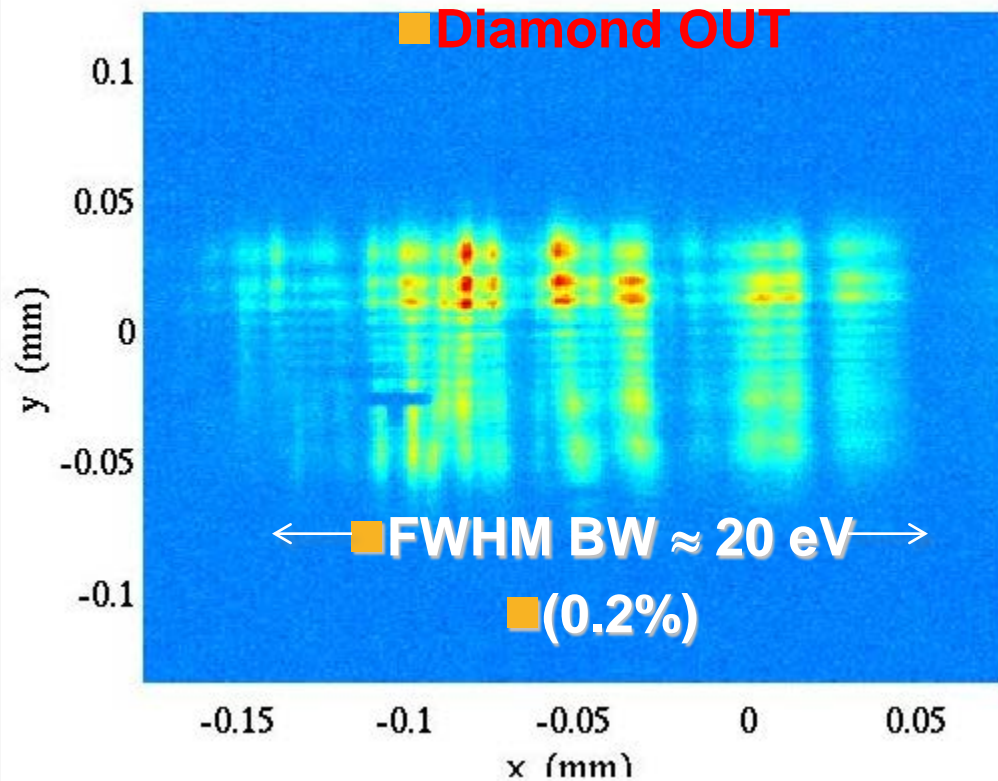


- Single-shot X-ray SASE spectrum compared with single-shot seeded spectrum at 0.15 nm for a 40pC electron bunch
- SASE spectrum includes all 28 undulators
- The seeding increases the spectral density of the FEL pulse.

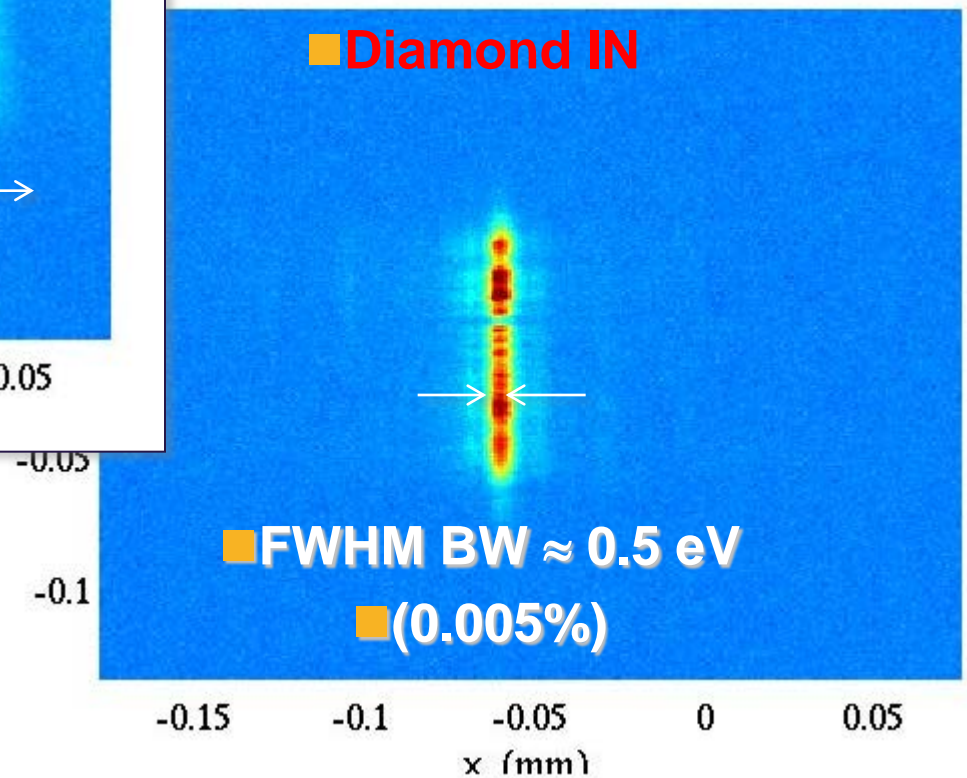
J. Amann et al., Demonstration of self-seeding in a hard-X-ray free-electron laser,
NATURE PHOTONICS DOI: 10.1038/NPHOTON.2012.180 (2012)

FEL Spectrum - SASE & Seeded

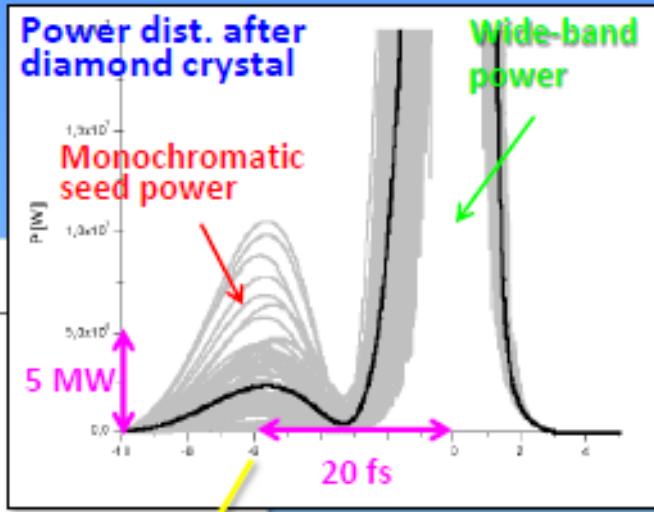
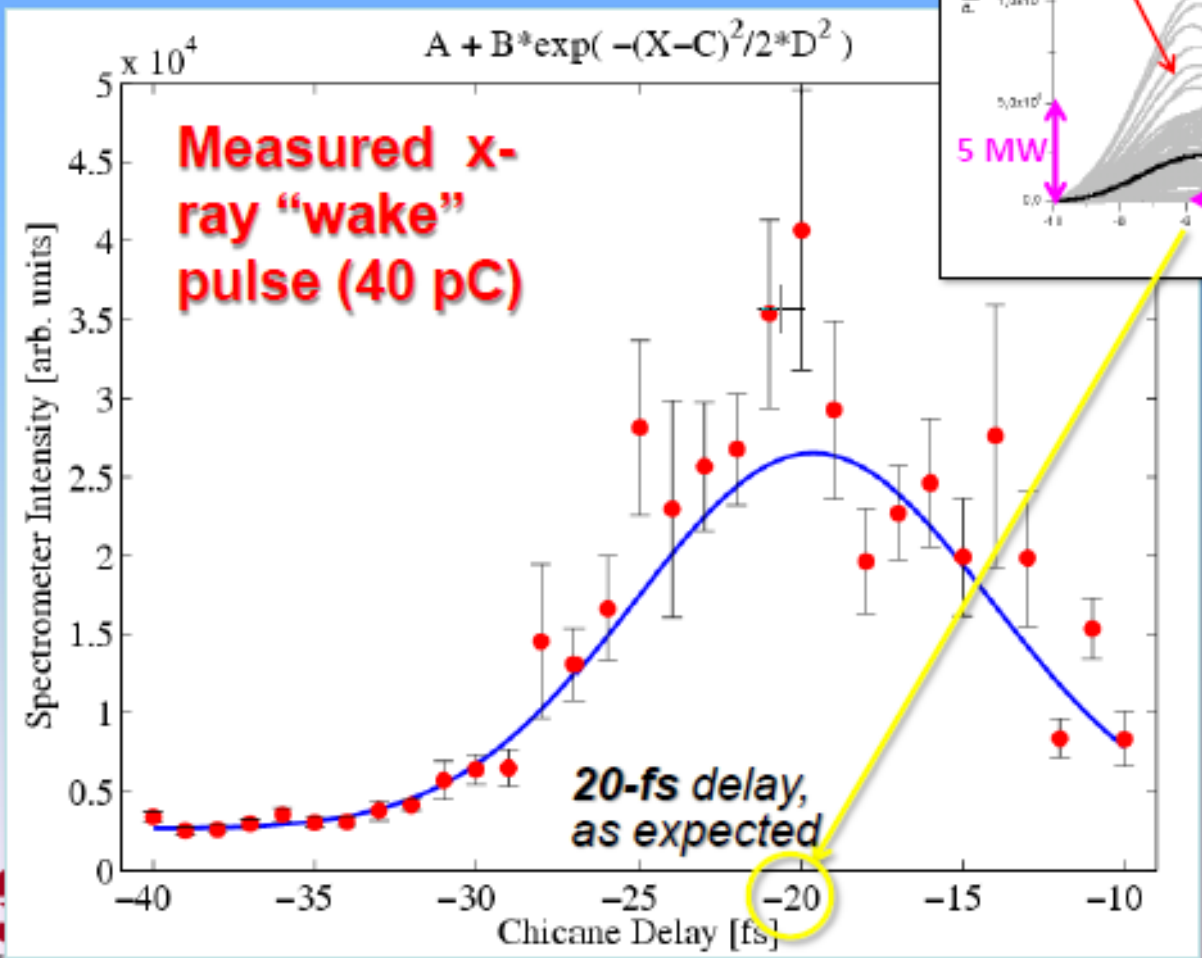
Profile Monitor XPP:OPAL1K:1 09-Jan-2012 19:36:24



Profile Monitor XPP:OPAL1K:1 10-Jan-2012 01:45:53



Chicane Delay Scan Shows X-Ray Wake Pulse



Geloni, Kocharyan, Saldin (DESY 10-133)



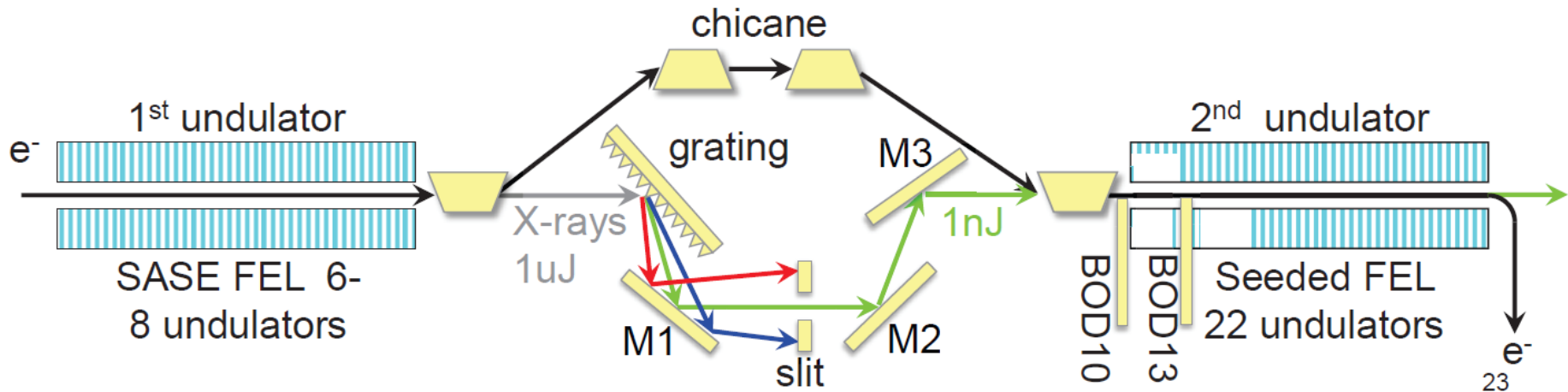


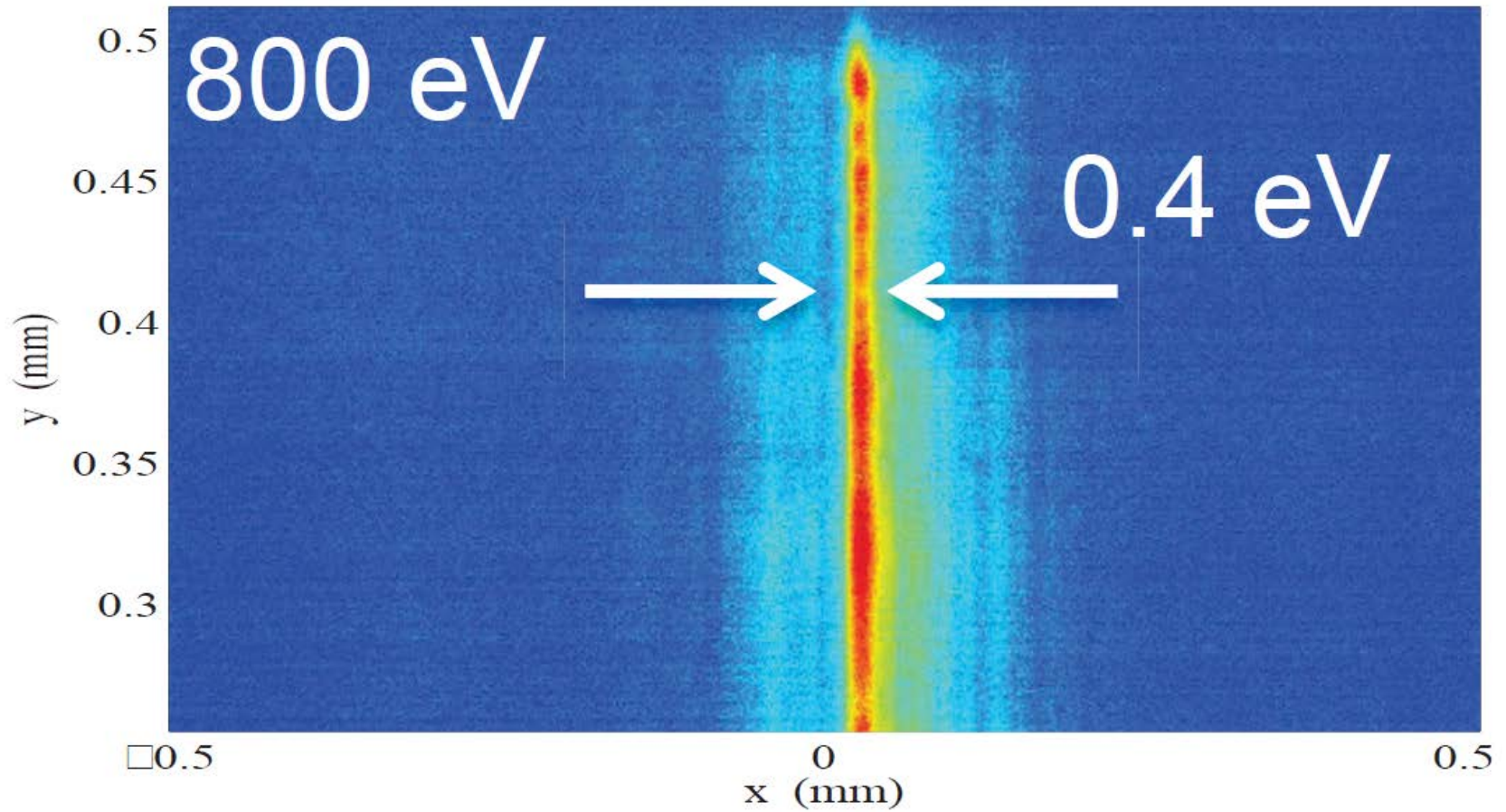
Demonstration of self-seeding in soft-X-ray free electron laser, D. Ratner, et al.

Phys. Rev. Lett, 114, 054801, 2015

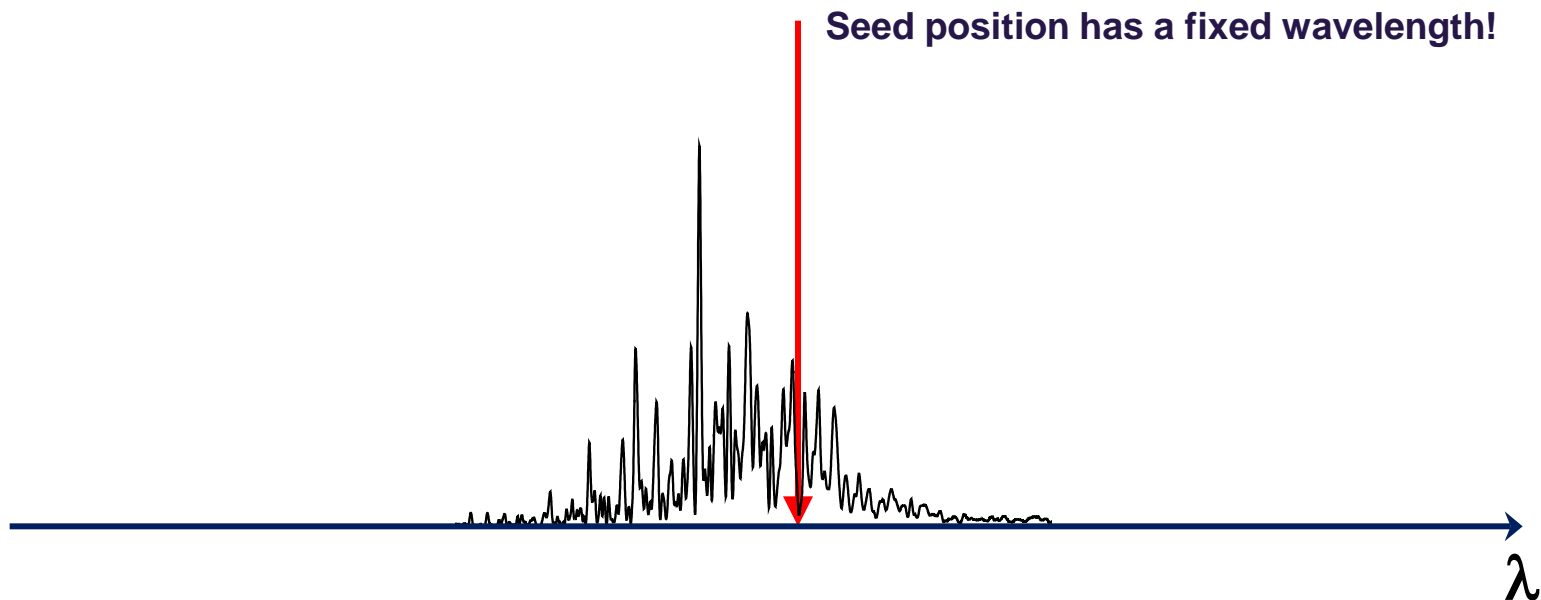
SXRSS

5 optical components and 2 diagnostics

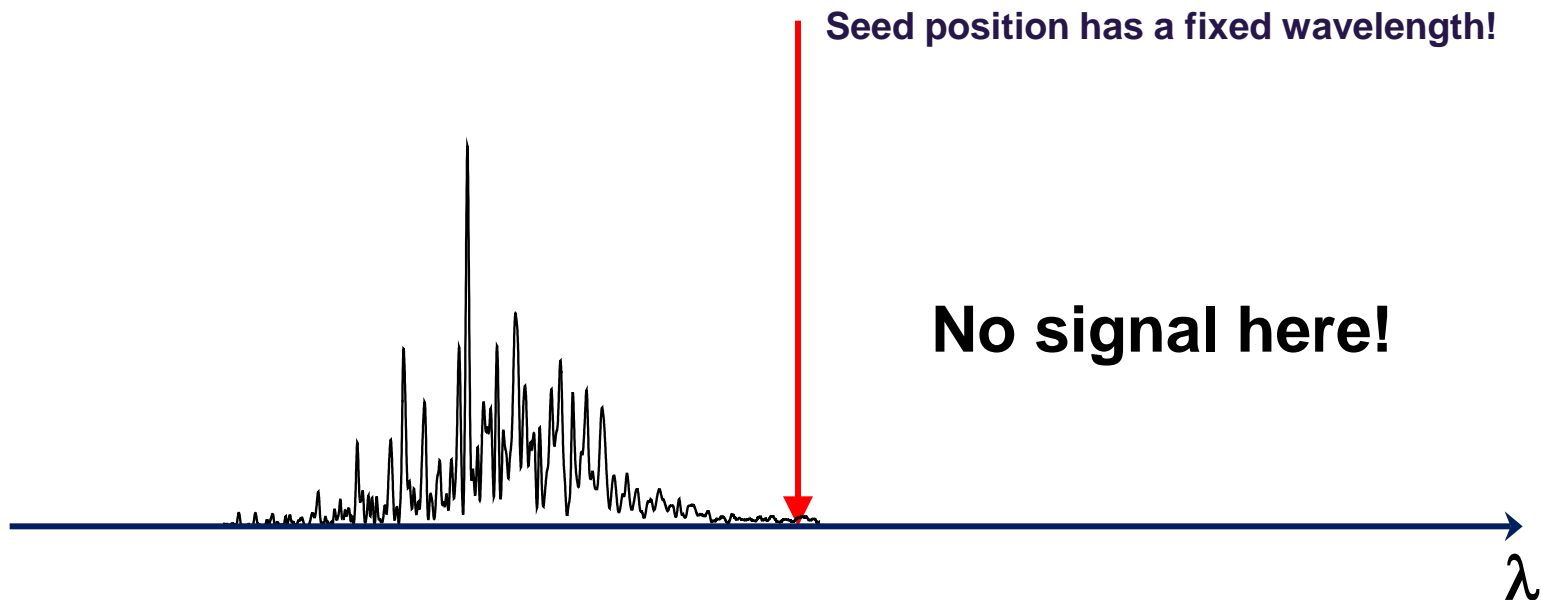




Self-seeding is sensitive to energy jitter of the electron beam at the LCLS



Self-seeding is sensitive to energy jitter of the electron beam at the LCLS



Self-seeding is sensitive to energy jitter of the electron beam at the LCLS

LCLS energy jitter: 0.04% ~ ρ !!

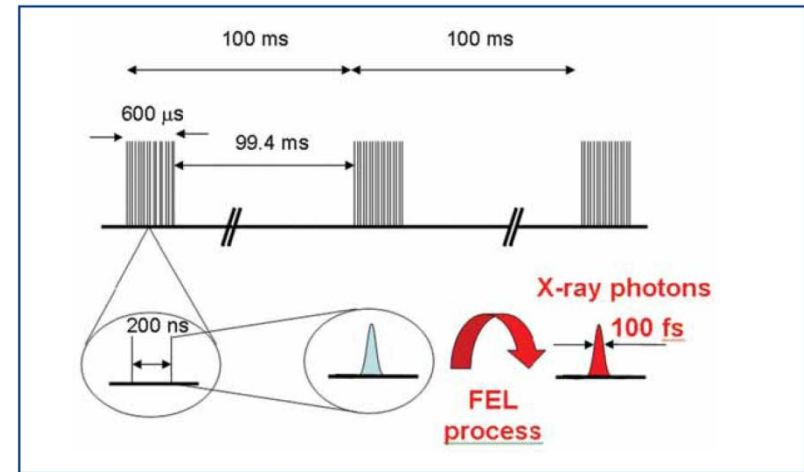
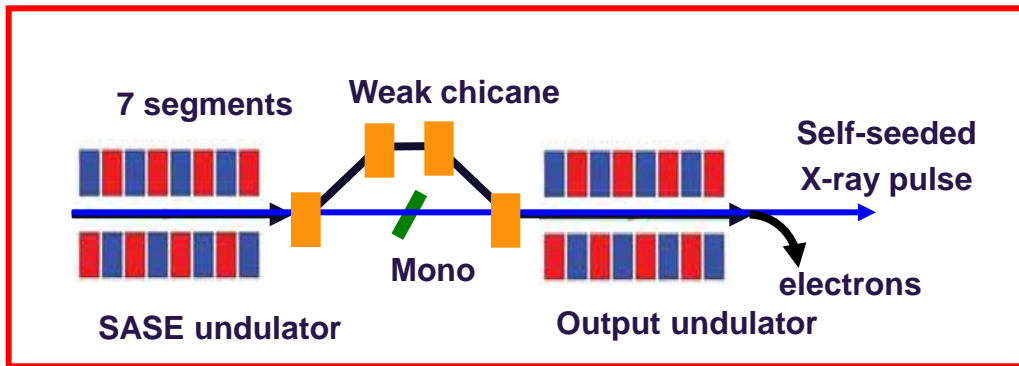
→ SASE spectral jitter ~ 0.08%

→ Need reduction to 0.02%

...it should not be a problem for the European XFEL
(jitter 0.01%)

1. Creation of transform-limited pulses through self-seeding at EXFEL
 2. Generation of TW X-ray pulses
 3. Schemes for variable X-ray polarization at EXFEL
 4. Possible THz pump/X-ray probe option at EXFEL
-

European XFEL pulse repetition rate ~ 27000 Hz \rightarrow
compromise in the first undulator length (heat loading!)



Energy per pulse 25pC/0.25nC bunch

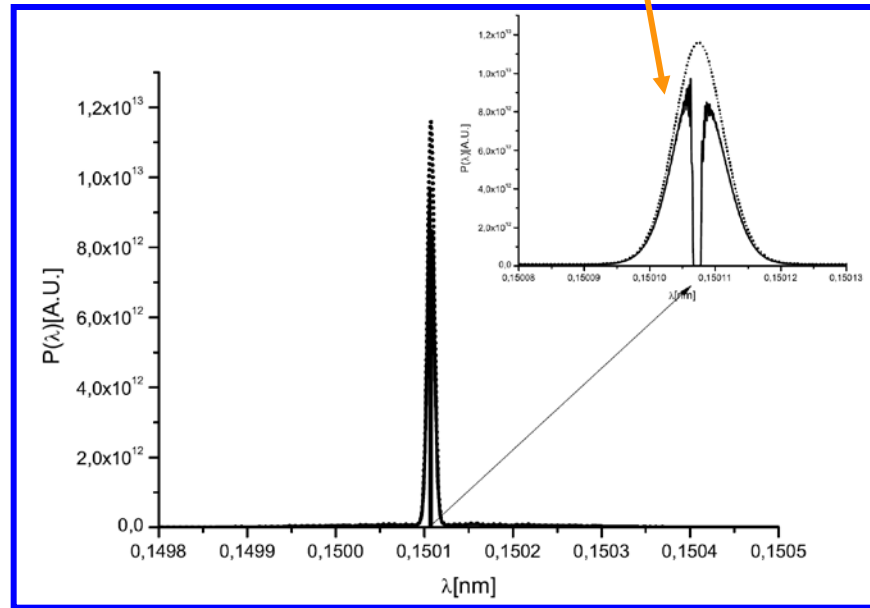
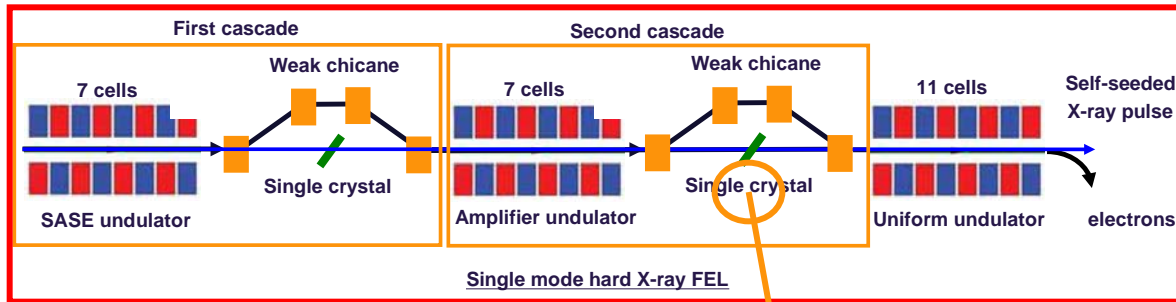
~ 150 -1500 nJ/pulse

\rightarrow Average incident power density at normal incidence within a train:

300 W/mm² (25pC) – 3000 W/mm² (0.25nC)

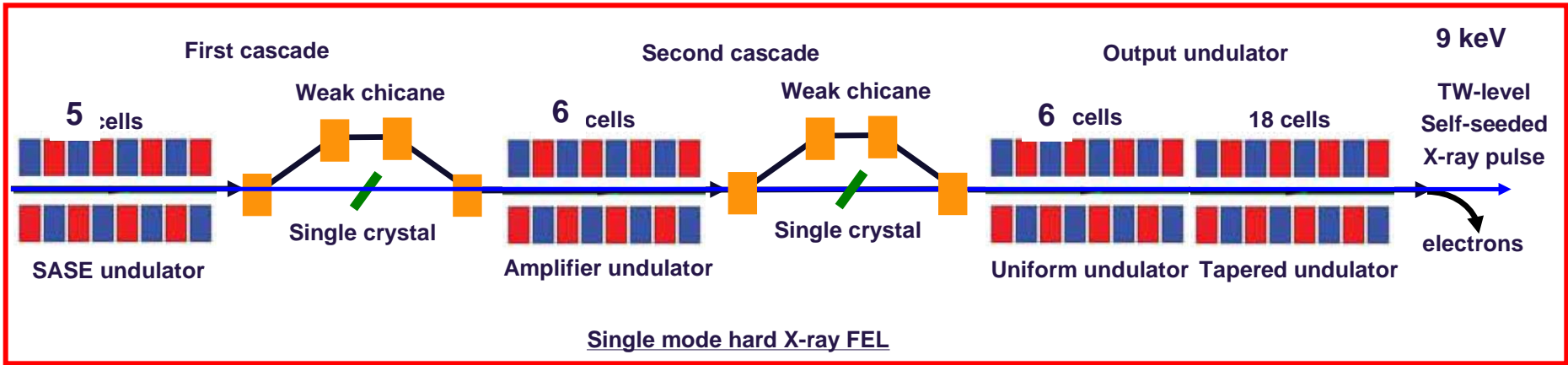
Solution: cascade self-seeding

Three-undulator setup

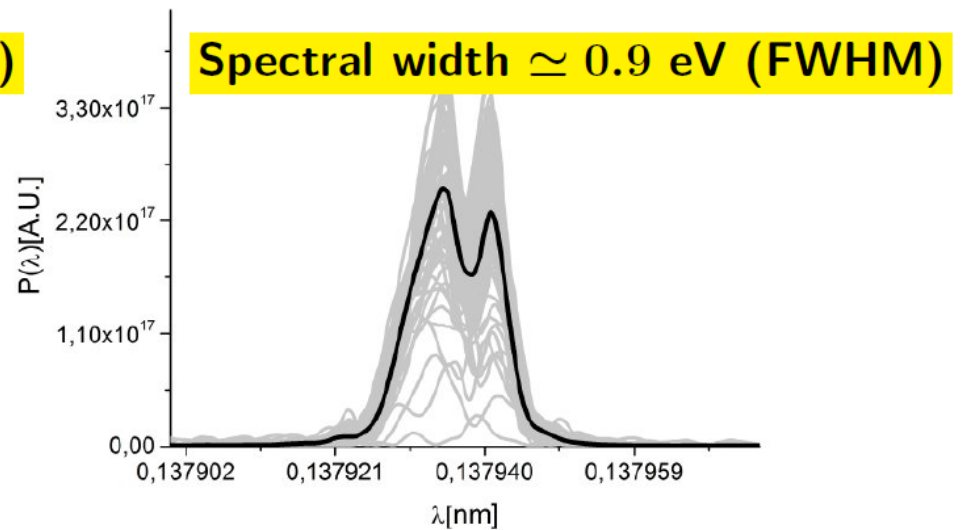
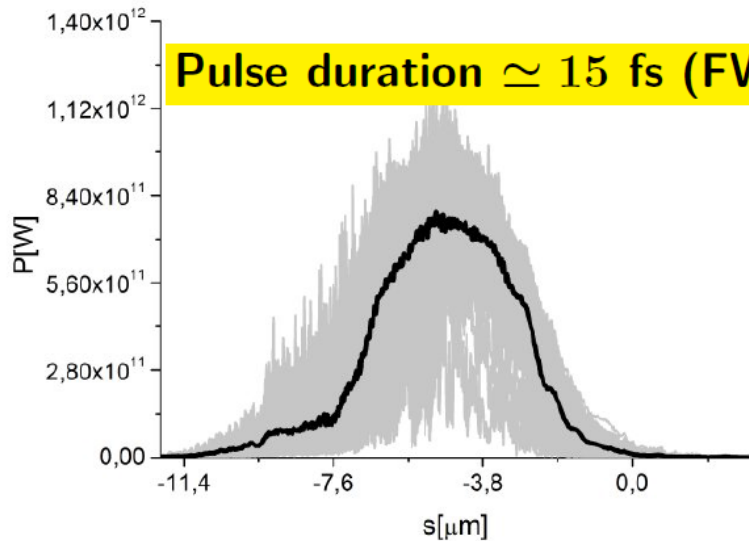
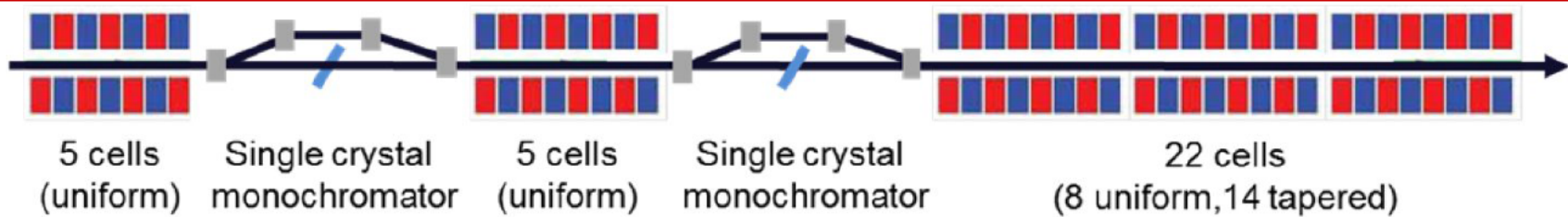


Small SASE contribution: at the second filter BW nearly Fourier limited already

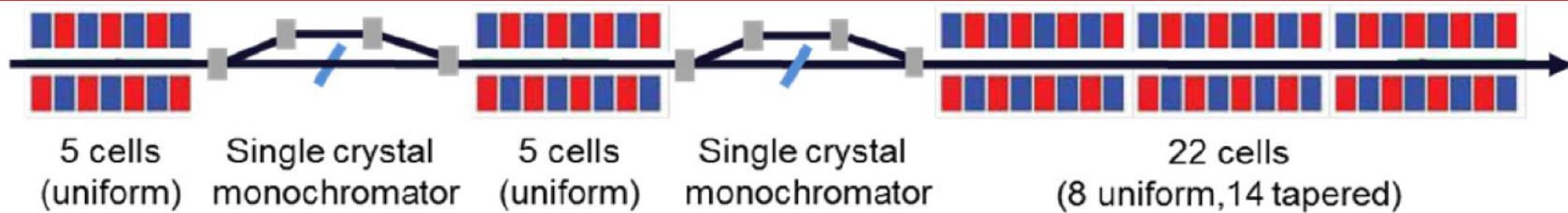
Solution: cascade self-seeding



Self-Seeding and Undulator Tapering for Highest Spectral Flux from the European XFEL



Self-Seeding and Undulator Tapering for Highest Spectral Flux from the European XFEL



Pulse energy $\simeq 10$ mJ

6.5×10^{12} ph/pulse @ 9.1 keV

Pulse duration $\simeq 15$ fs (FWHM)

Spectral width $\simeq 0.9$ eV (FWHM)

Beam diameter $\simeq 50$ μm (FWHM)

Beam divergence $\simeq 2$ μrad (FWHM)

Peak sp. flux 6×10^9 ph/meV/pulse

Average sp. flux 2×10^{14} ph/meV/s

$\simeq 10^3 - 10^4$ -times more than at synchrotrons



High-repetition-rate seeded XFELs

Features

$\simeq 10^4$ times more spectral
flux than at storage ring sources

Science

ultra-high-resolution spectroscopies

Novel opportunities for sub-meV inelastic X-ray scattering experiments at the European XFEL

Oleg Chubar,^a Gianluca Geloni,^b Vitali Kocharyan,^c
Anders Madsen,^b Evgeni Saldin,^c Svitozar Serkez,^c
Yuri Shvid'ko^d and John Sutter^e

^a*Brookhaven National Laboratory, New York, United States*

^b*European XFEL GmbH, Hamburg, Germany*

^c*Deutsches Elektronen-Synchrotron (DESY), Hamburg, Germany*

^d*Argonne National Laboratory, Argonne, United States*

^e*Diamond Light Source Ltd, Didcot, Oxfordshire OX11 0DE, UK*

IXS is challenging!

The smaller ΔE is required, the higher indexed Bragg reflection at higher photon energy E has to be used.

Example: $\Delta E = 0.1 \text{ meV}$ requires $E = 31 \text{ keV}$

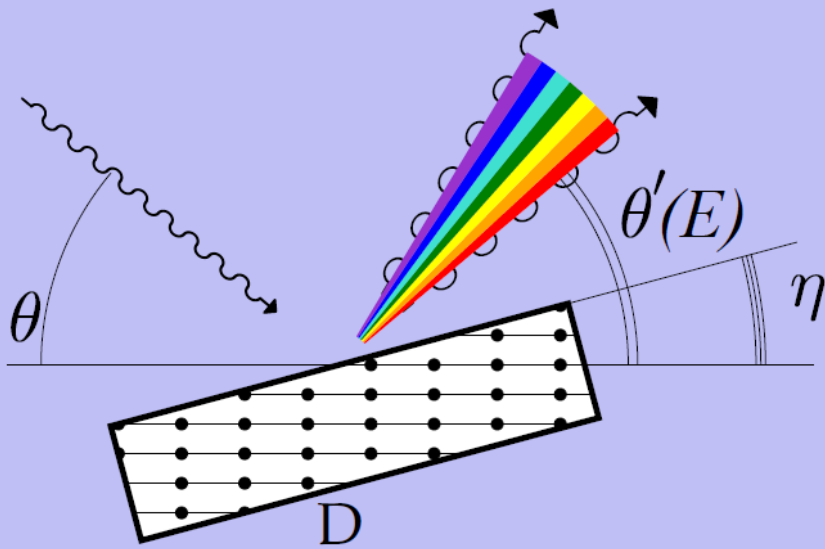
Low flux & countrates,
time-consuming experiments:

for $\simeq 10^9$ incident photons
only $\simeq 1$ scattered photon
in the detector



Angular Dispersion

An asymmetrically cut crystal behaves like a diffraction grating dispersing photons with different photon energies: **effect of angular dispersion.**



M. Kuriyama and W.J. Boettinger, *Acta Cryst.*, A32 (1976) 511

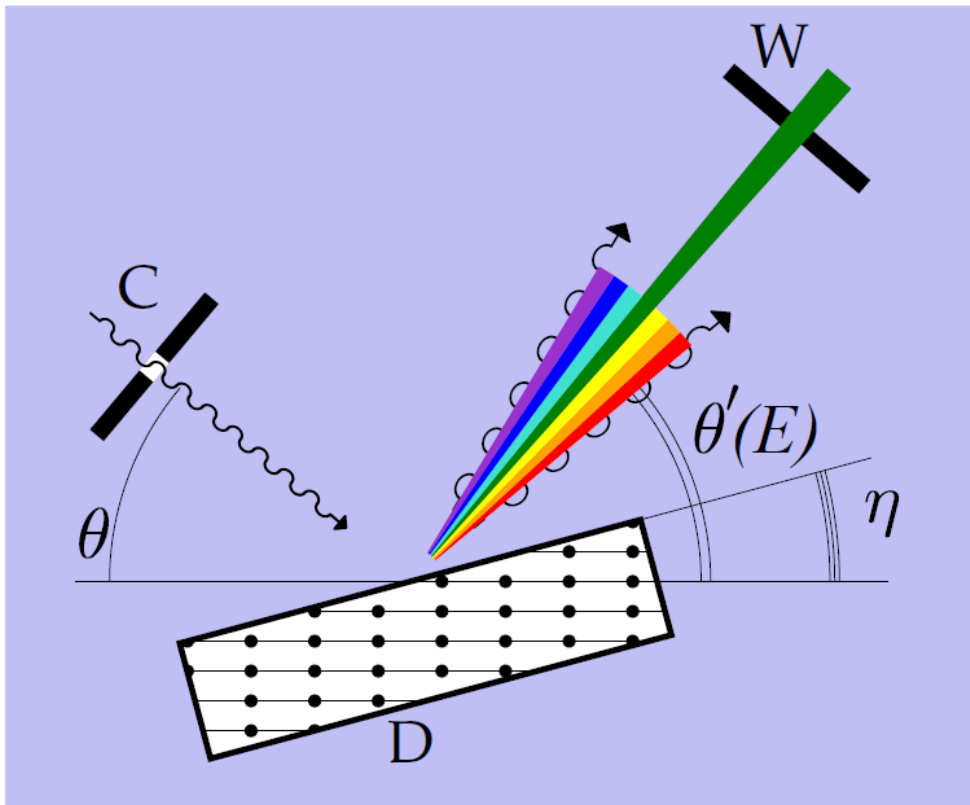
T. Matsushita and U. Kaminaga, *J. Appl. Crystallogr.*, 13 (1980) 472

Yu. Shvyd'ko, *X-Ray Optics*, Springer-Verlag (2004)



Angular Dispersion

An asymmetrically cut crystal behaves like a diffraction grating dispersing photons with different photon energies: **effect of angular dispersion.**



C - collimator

D - dispersing element

W - wavelength selector

Yu. Shvyd'ko, *X-Ray Optics*, Springer-Verlag (2004)

Angular dispersion: overcoming limitations set by the Darwin width.

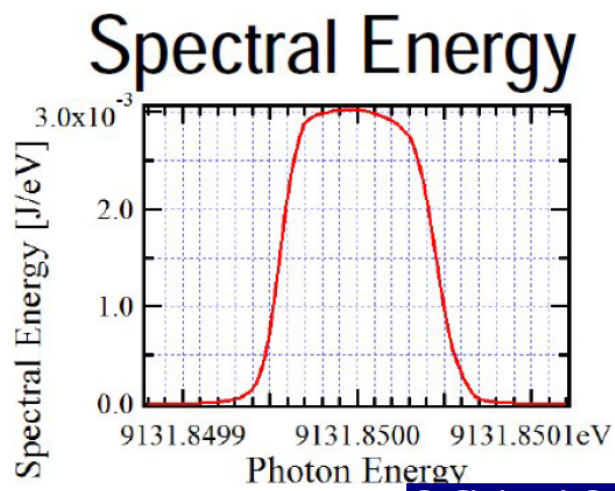
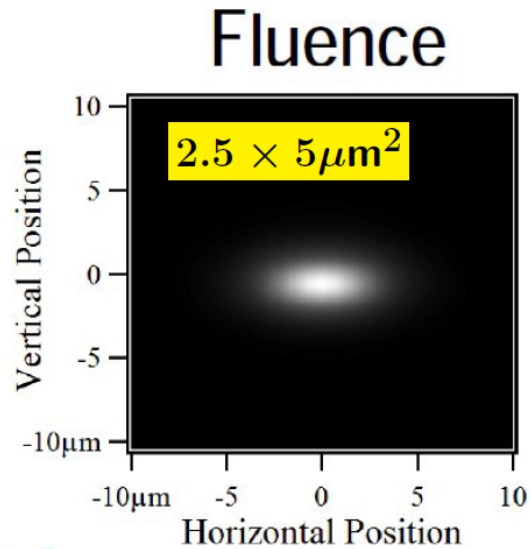
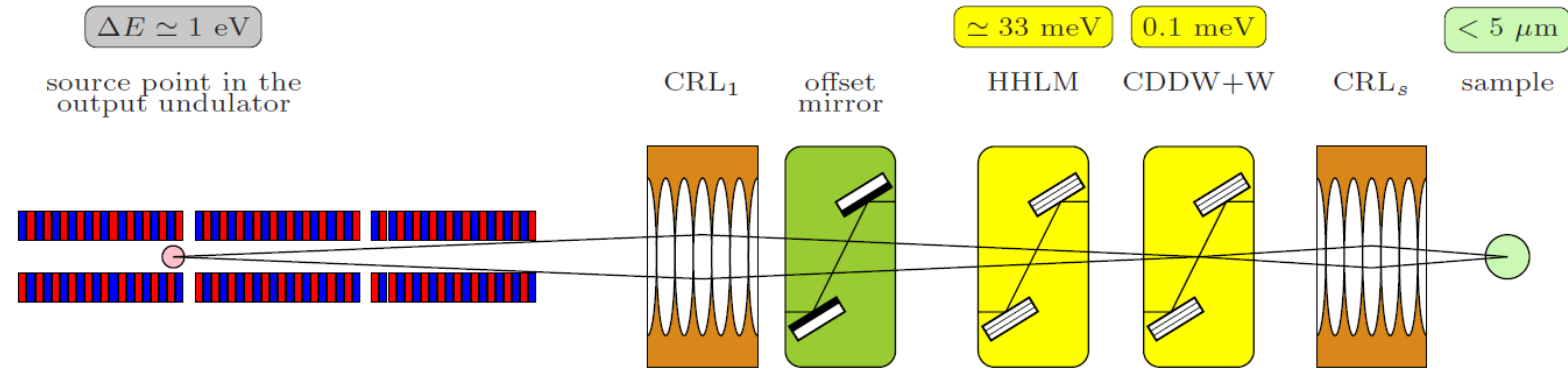


A proof-of-principle x-ray spectrometer for ultra-high-resolution IXS applications (UHRIX) has been developed, built, and recently tested at the APS

The work is in progress to demonstrate an IXS spectrograph with 0.1 meV and $\lesssim 0.1 \text{ nm}^{-1}$ resolution.

UHRIX utilizes 9 keV x-ray photons. It is applicable therefore at XFEL facilities.

Wafront Propagation of the XFEL Pulse Through X-ray Optic to the Sample



Energy: $0.27 \mu\text{J} \Rightarrow 2 \times 10^8 \text{ ph/pulse}$

Bandwidth: 0.09 meV

Average sp. flux: $6 \times 10^{13} \text{ ph/meV/s}$

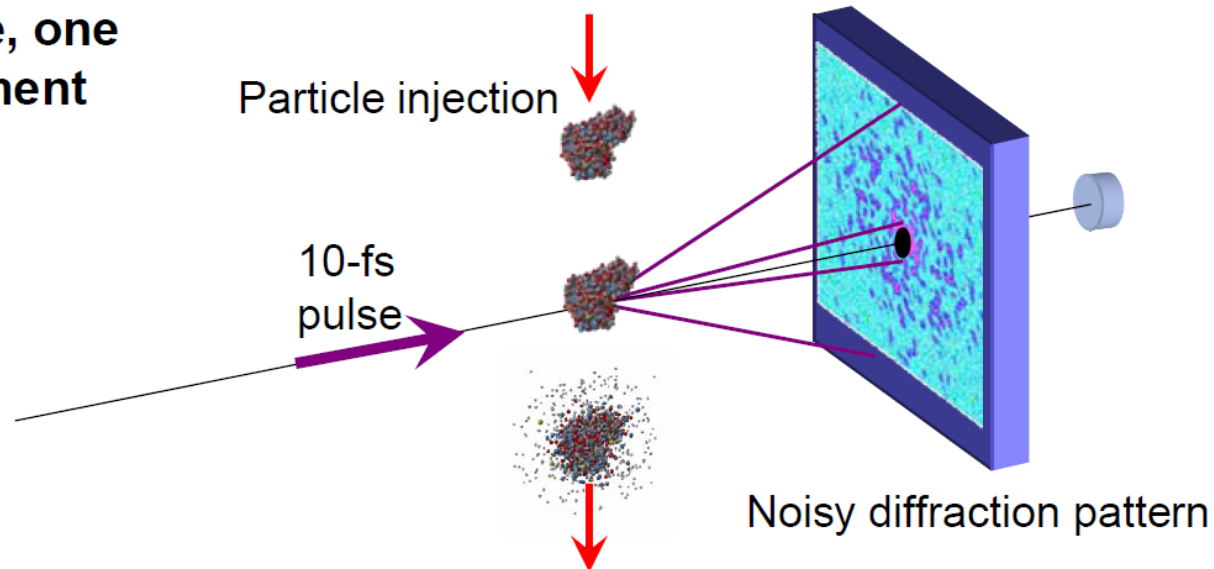
$> 10^3$ than at the APS

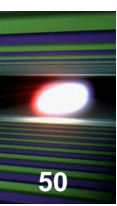
THEORY predicts XFELs may allow high resolution imaging of single particles / molecules

Neutze, Wouts, van der Spoel, Weckert, Hajdu *Nature* 406, 752-757 (2000)

X-ray free-electron lasers may enable atomic-resolution imaging of biological macromolecules

One pulse, one measurement





Imaging of a single protein molecule...

...can we solve this problem at European XFEL in its baseline configuration?

Perspectives for Imaging Single Protein Molecules with the Present Design of the European XFEL

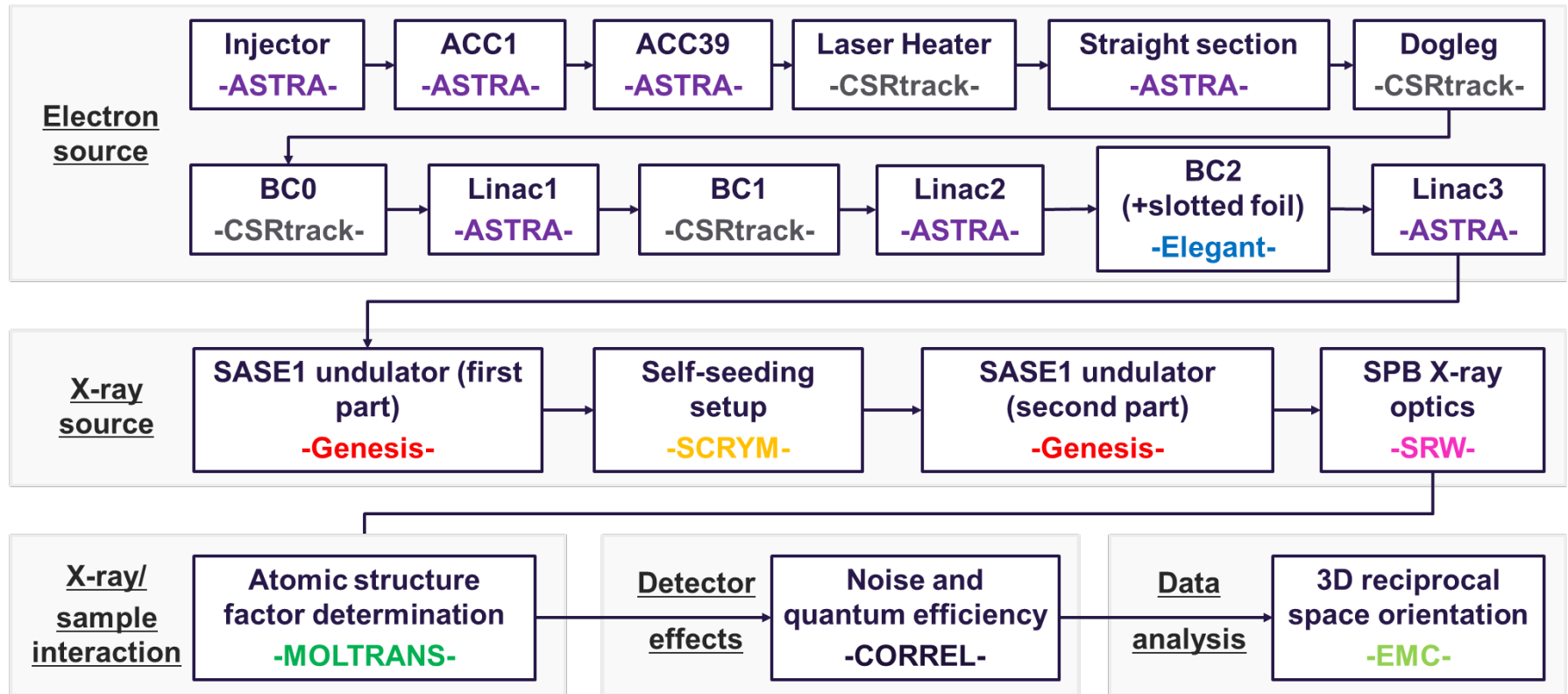
Kartik Ayyer,¹ Gianluca Geloni,² Vitali Kocharyan,³ Evgeni Saldin,³ Svitozar Serkez,³ Oleksandr Yefanov,¹ and Igor Zagorodnov³

¹) *Center for Free-Electron Laser Science, Hamburg, Germany*

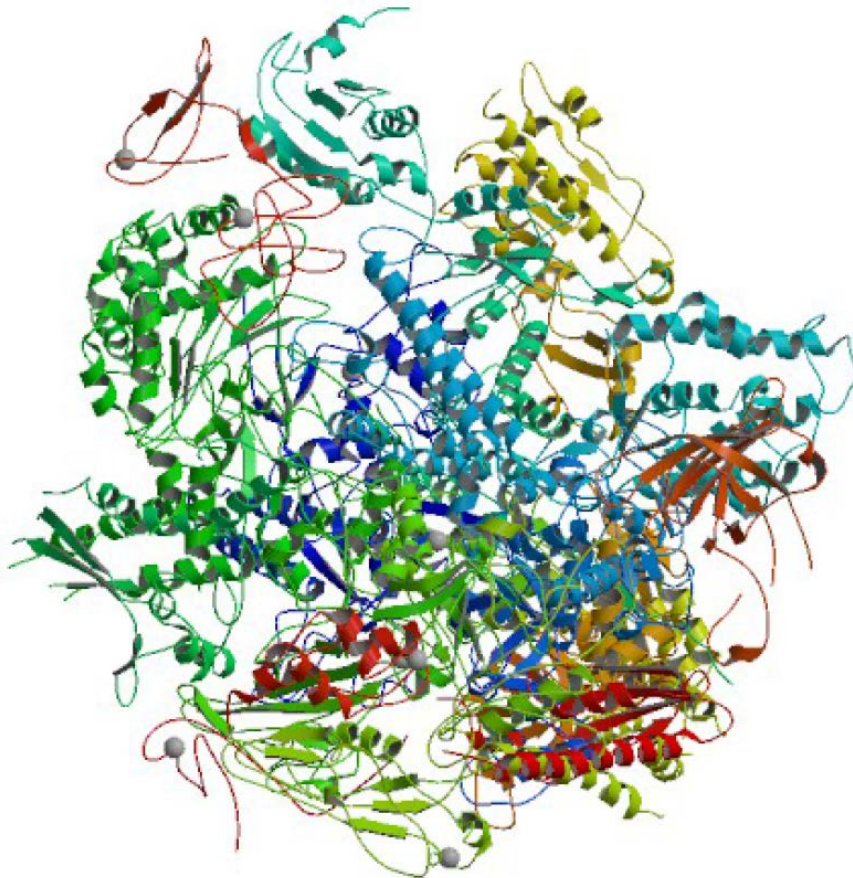
²) *European XFEL GmbH, Hamburg, Germany*

³) *Deutsches Elektronen-Synchrotron (DESY), Hamburg, Germany*

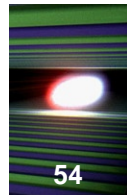
Simulations Flowchart



In this talk: consider one case study



- RNA Pol II size w ~ 15 nm
- 30000 atoms
- Wanted resolution : 0.4 nm

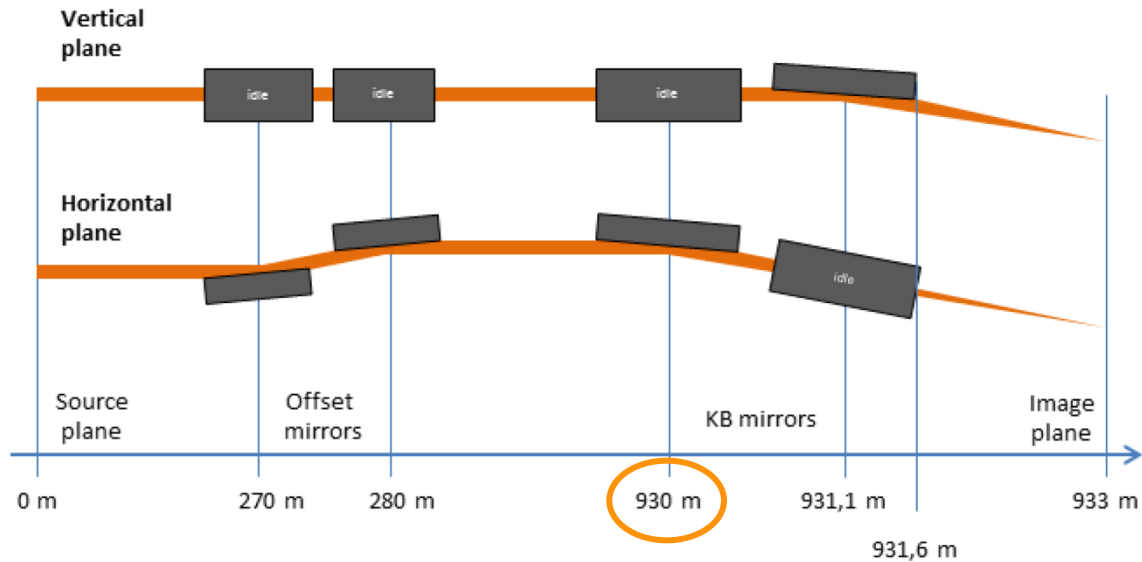


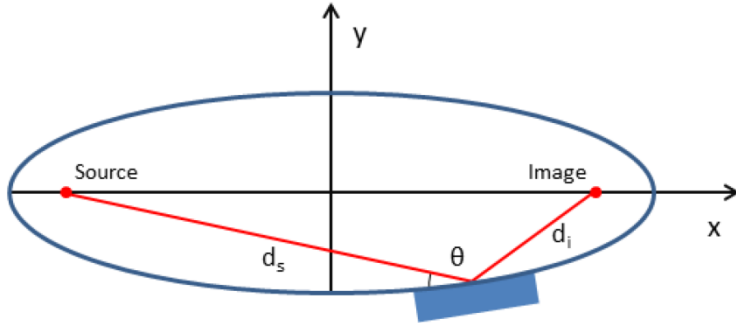
- Object with width $w \rightarrow$ speckles of minimal size $2\pi/w$
- Shannon interval $\Delta q_s = \pi/w$
- Average #photons per $\Omega_p \sim \lambda^2/(2\pi)^2(\Delta q_s)^2 = \lambda^2/(2w)^2 :$

$$\langle N_p \rangle = F \cdot P \cdot r_e^2 N_{\text{atom}} |f|^2 \frac{\lambda^2}{4w^2}$$

- For our molecule: $F=10^{13}$ ph/(100 nm)² $\rightarrow \langle N_p \rangle \sim 1.5$ per Shannon pixel at 4 keV
- To avoid damage: $\sim < 5$ fs long. Here we assume 4fs
- $F=10^{13}$ ph/(100 nm)², **4fs pulse, 4keV** $\rightarrow 6\text{mJ} \rightarrow$ **1.5 TW**
- **Note: 1TW at 4keV gives the same #ph as 27 TW at 12 keV!**

- Available with baseline SASE FELs: order of 100 GW vs. needed: 1.5 TW → **Self-seeding + Tapering?**
- Also, we need to transport and focus:





KB system: 100nm spot size (ok for $w \sim 15\text{nm}$)
 Elliptical mirror \rightarrow only one working angle without aberrations

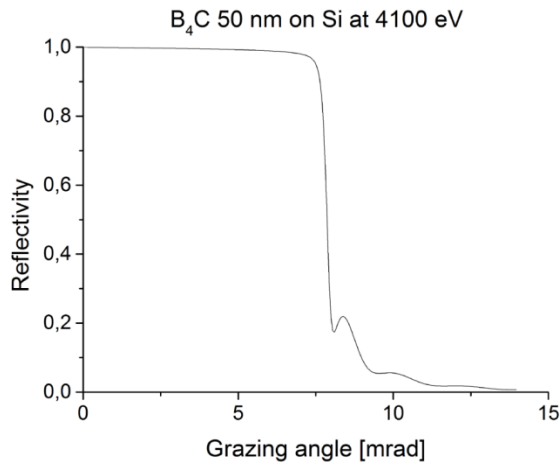
- Selected angle: 3.5 mrad

B_4C coating between 3keV and 7keV

Ru coating between 7keV and 16 keV

- 950mm clear aperture @ 3.5mrad

\rightarrow 3.3 mm available lateral aperture

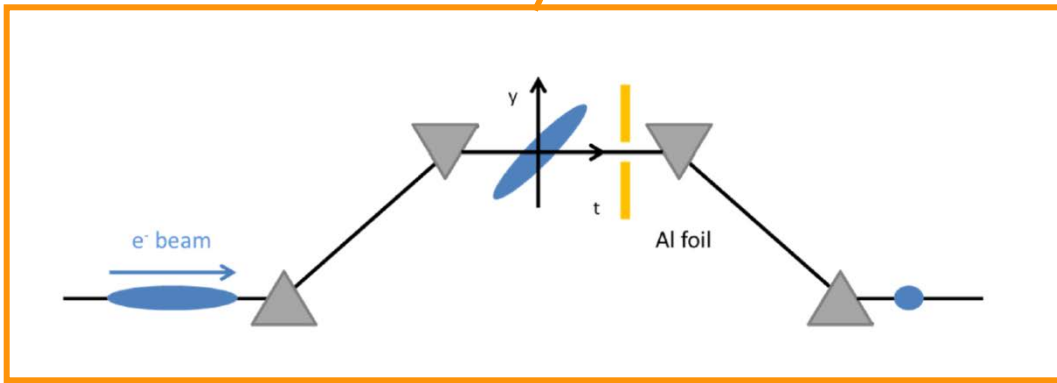
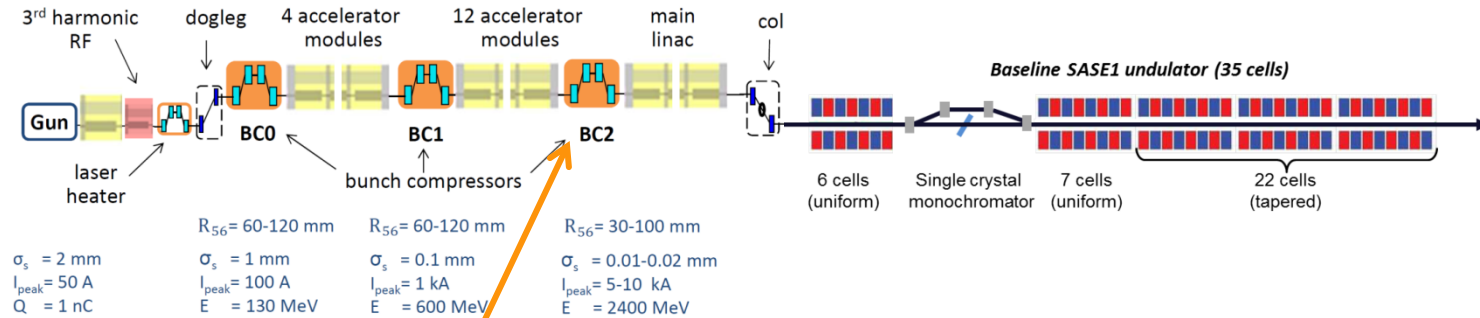


BUT

4fs photon pulse pulse length \rightarrow 20pC charge \rightarrow
 lowest emittance \rightarrow shortest gain length \rightarrow largest
 divergence $\sim 5\mu\text{rad}$ FWHM @ 4keV

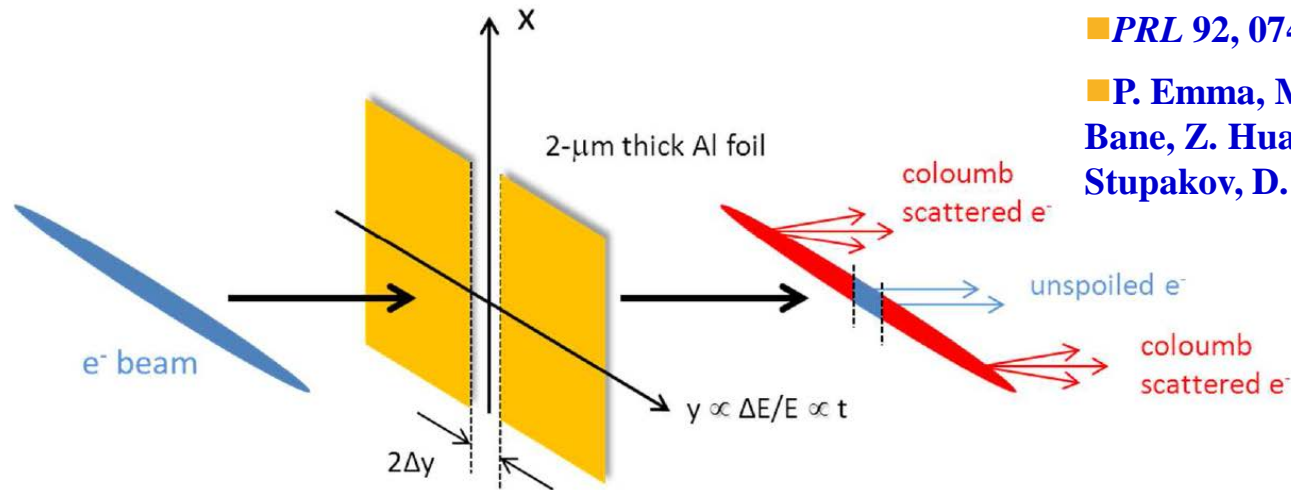
900m x $5\mu\text{rad}$ x 1.7~8mm required lateral aperture

HXRSS with special accelerator mode of operation



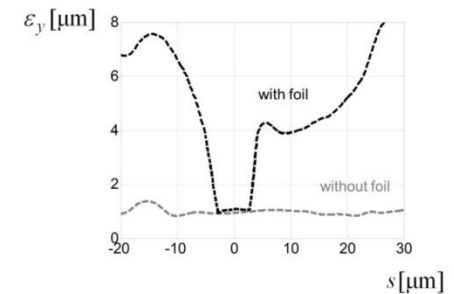
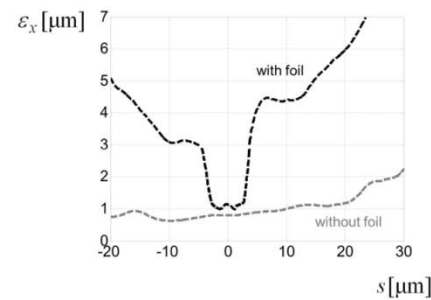
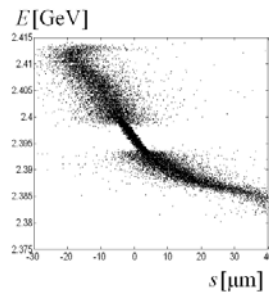
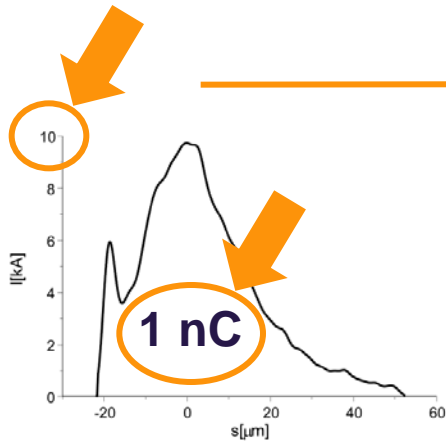
Insert a slotted foil in the last chicane (method invented and experimentally proven at the LCLS)

- [PRL 92, 074801 \(2004\).](#)
- [P. Emma, M. Cornacchia, K. Bane, Z. Huang, H. Schlarb, G. Stupakov, D. Walz \(SLAC\)](#)



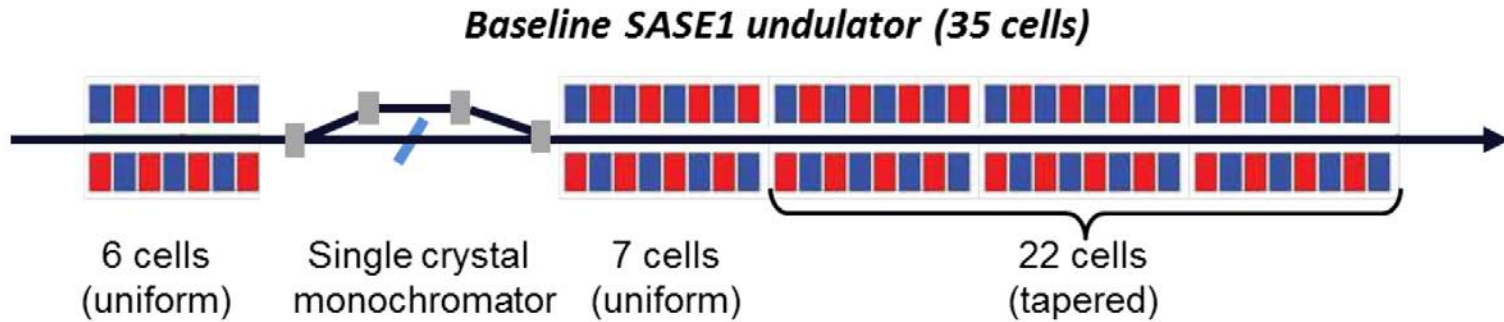
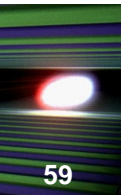
■ *PRL* 92, 074801 (2004).

■ P. Emma, M. Cornacchia, K. Bane, Z. Huang, H. Schlarb, G. Stupakov, D. Walz (SLAC)

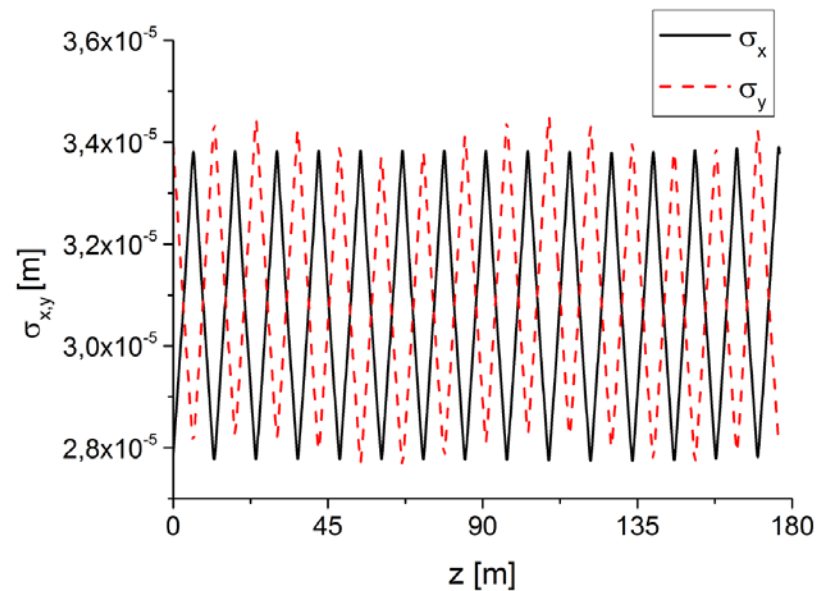


Advantage: pulse duration tunable decoupled from charge and hence from divergence. Here: 4fs and 12fs radiation pulse length

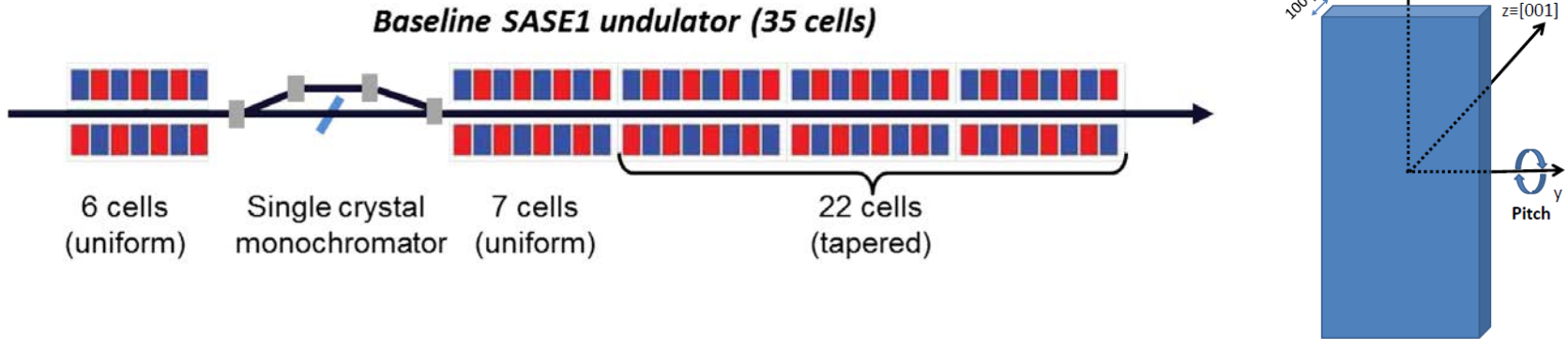
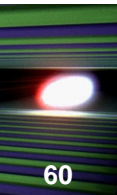
Self-seeding HXRSS setup



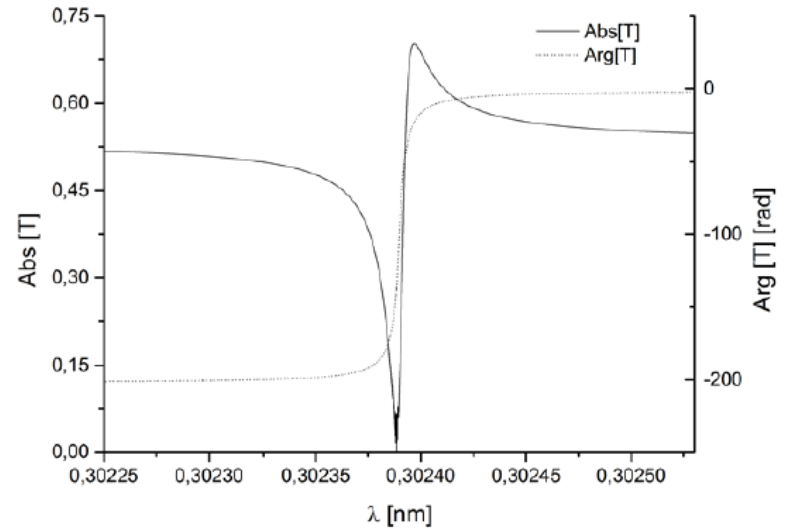
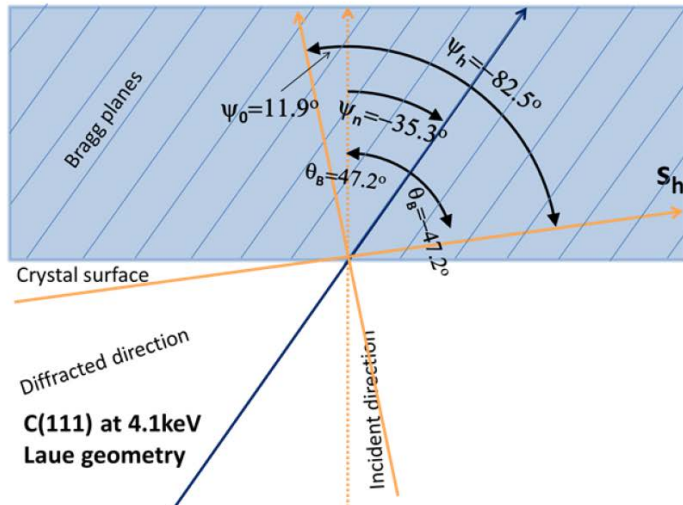
	Units	
Undulator period	mm	40
Periods per cell	-	125
Total number of cells	-	35
K parameter (rms)	-	3.217
Intersection length	m	1.1
Wavelength	nm	0.302
Energy	GeV	14
Charge	nC	1

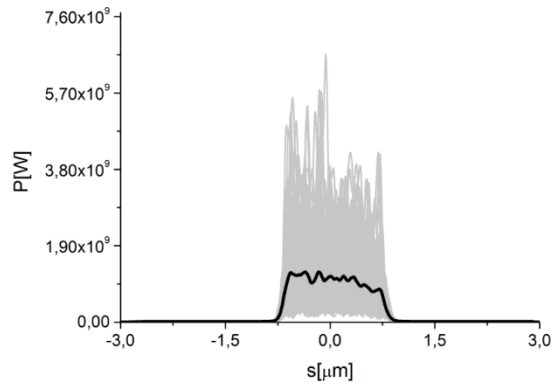


Self-seeding HXRSS setup

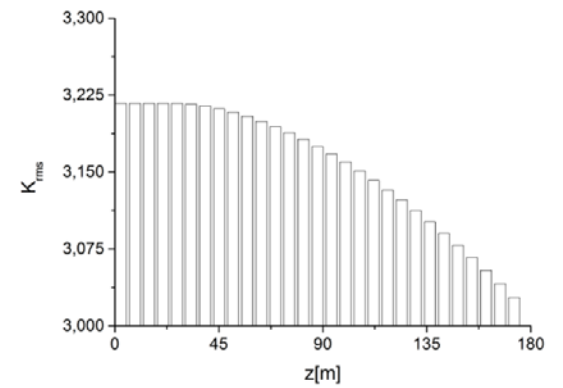
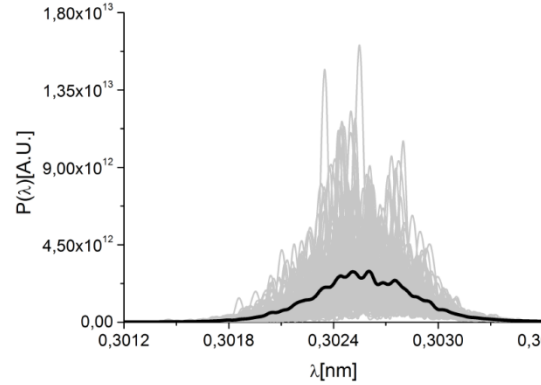


Assumes a crystal arrangement similar to that at the LCLS

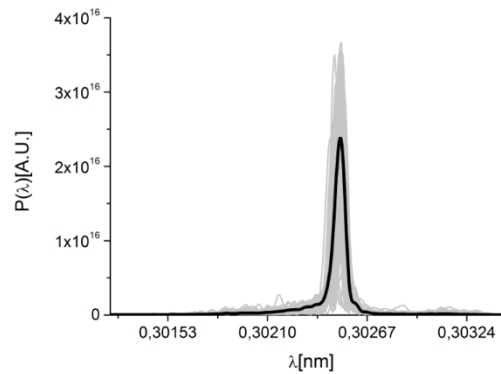
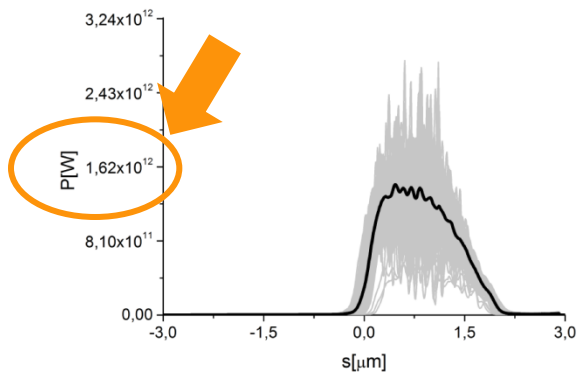




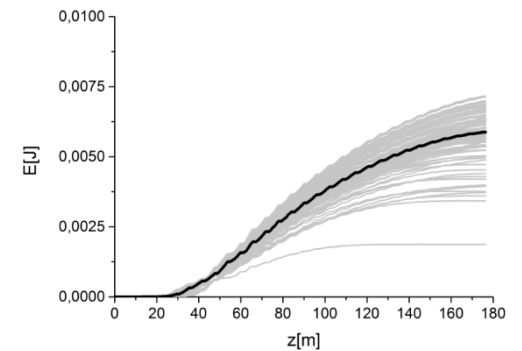
At the crystal



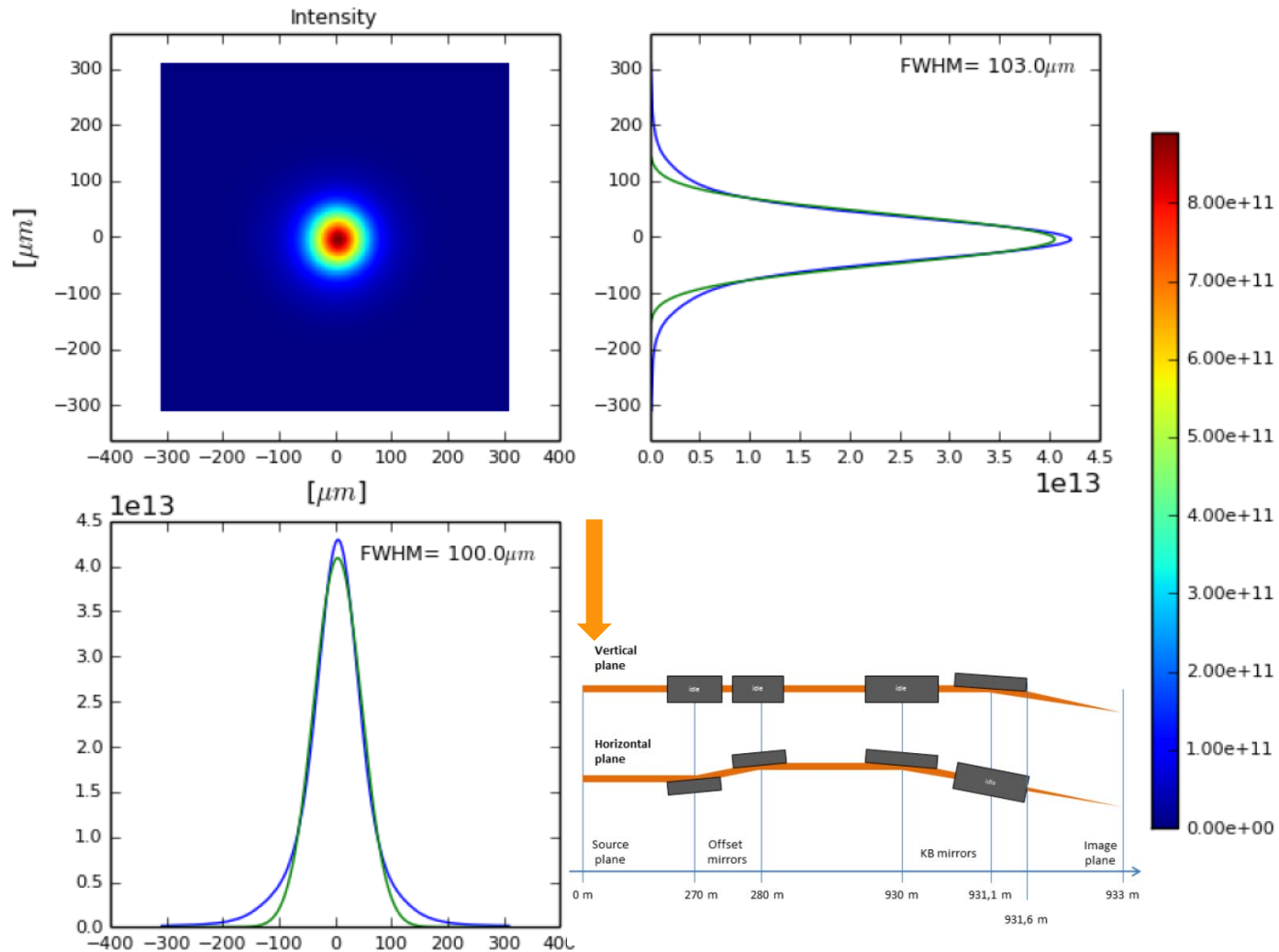
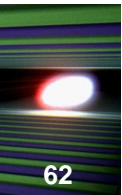
Tapering law



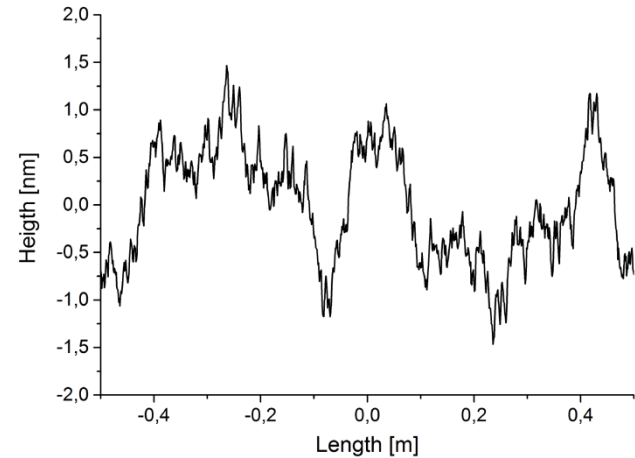
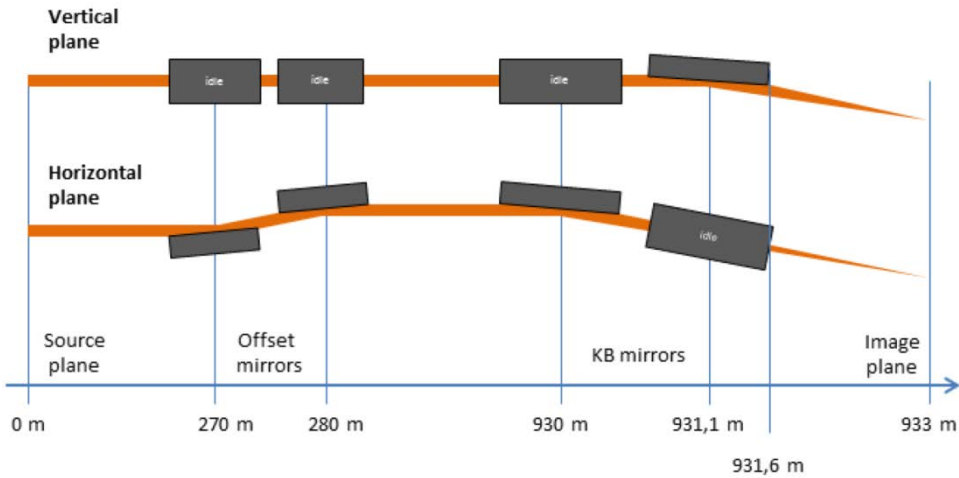
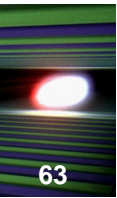
Output



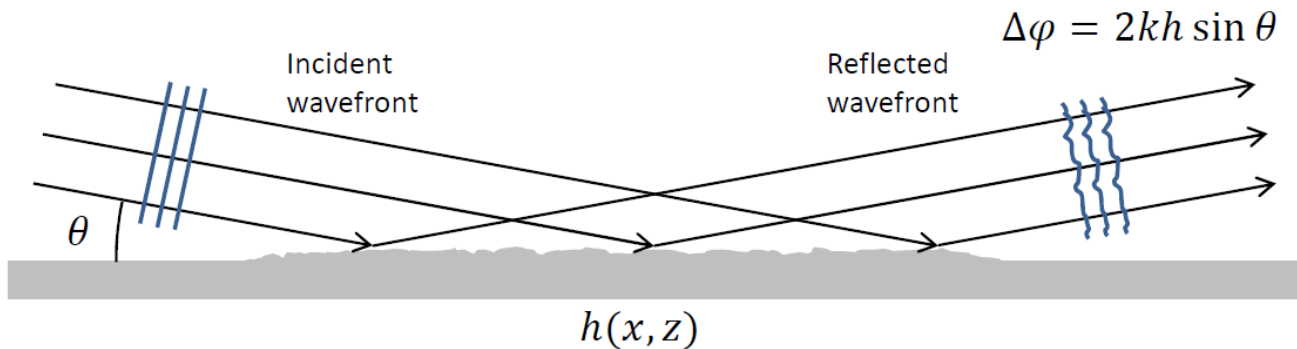
Wavefront propagation: Source, 26m before the undulator exit



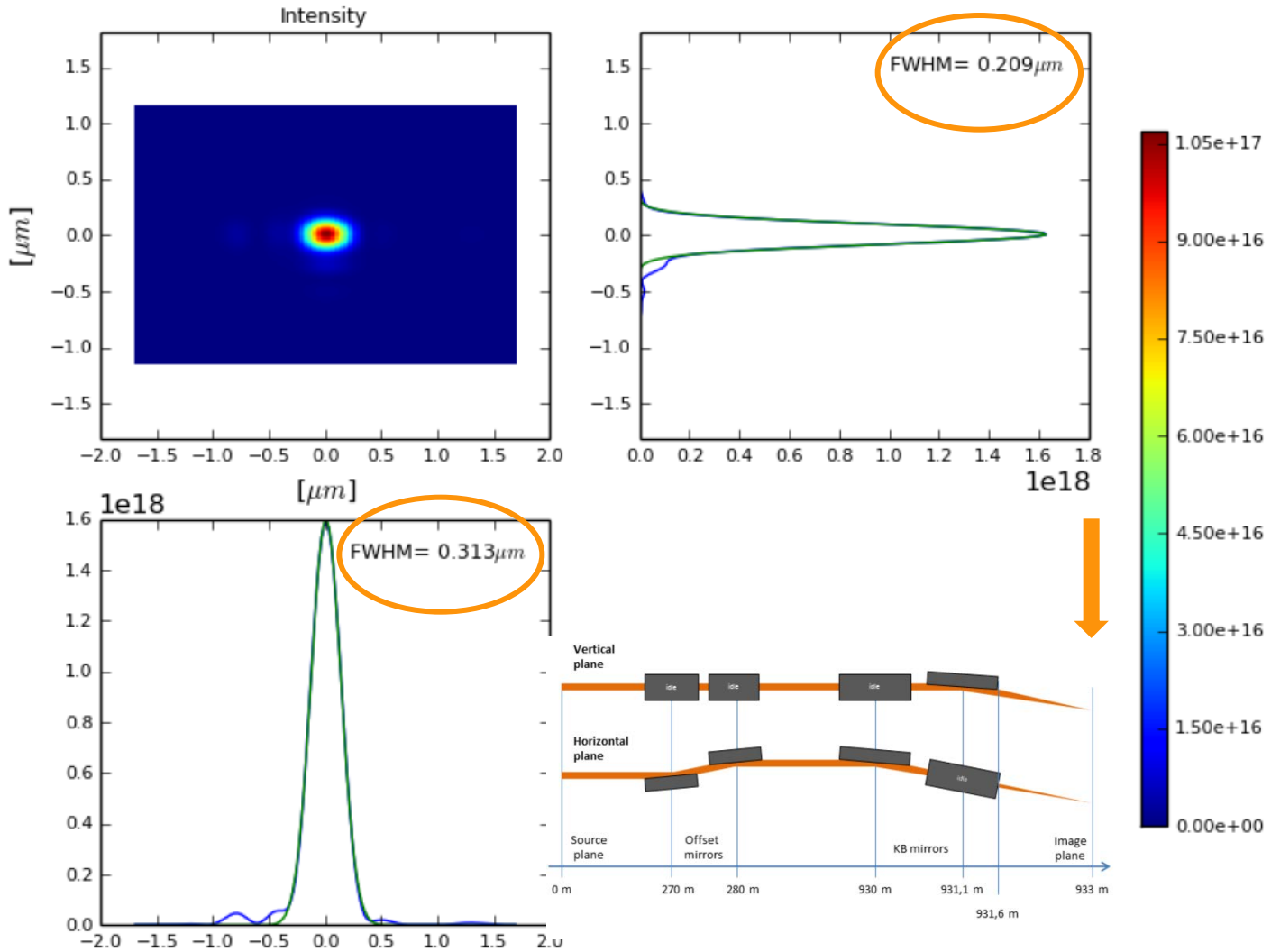
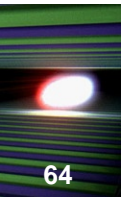
Mirror roughness

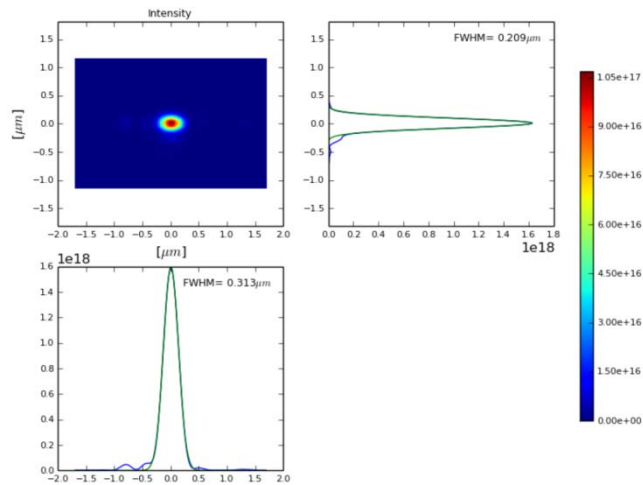


$$2h_{\text{rms}}\theta_i \sqrt{N} < \lambda/14 \rightarrow \text{rms height} \sim 1\text{nm}$$



Wavefront propagation: at the focus





$$F = N_p/S$$

$$N_p \sim 10^{13}$$

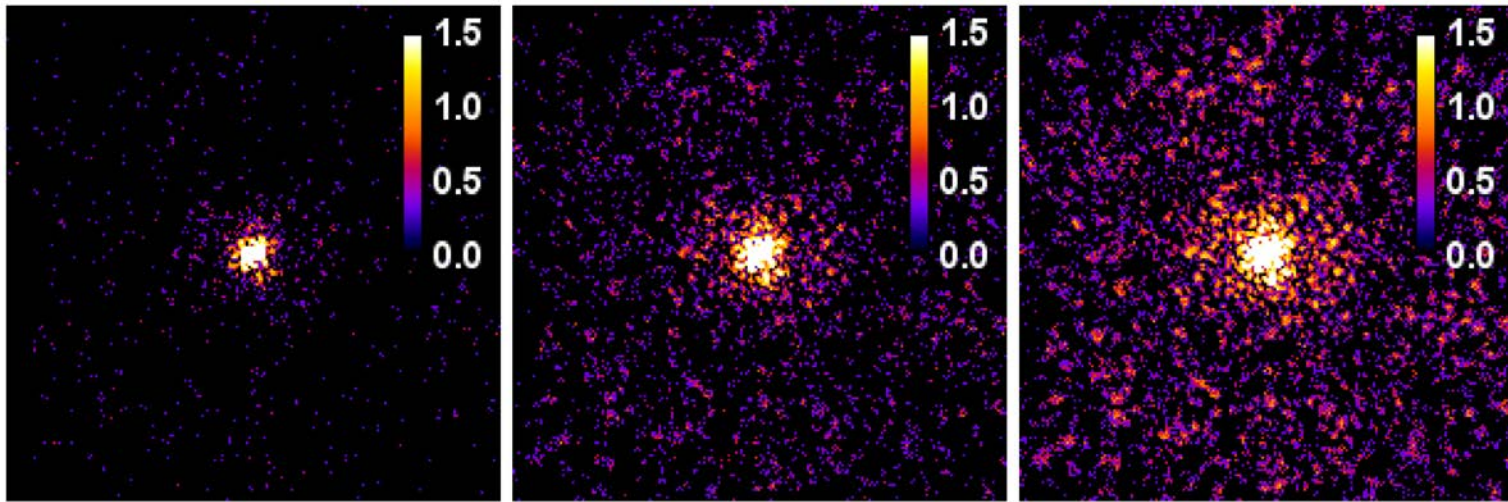
$$\frac{1}{S} = \frac{\max(W)}{\int W(x, y) dx dy} \sim 1.5 \cdot 10^9 \text{ cm}^{-2}$$

→ At present design

→ $F \sim 1.5 \cdot 10^{22} \text{ ph/cm}^2$

This fluence we used in our simulations
of data processing

Simulated diffraction data from the test object



$F \sim 1.5 \cdot 10^{22}$ ph/cm²

$F \sim 0.5 \cdot 10^{23}$ ph/cm²

$F \sim 1.0 \cdot 10^{23}$ ph/cm²

E photons = 4.1 keV.

Detector: 200 mm by 200 mm in size

Detector location: 100 mm from sample.

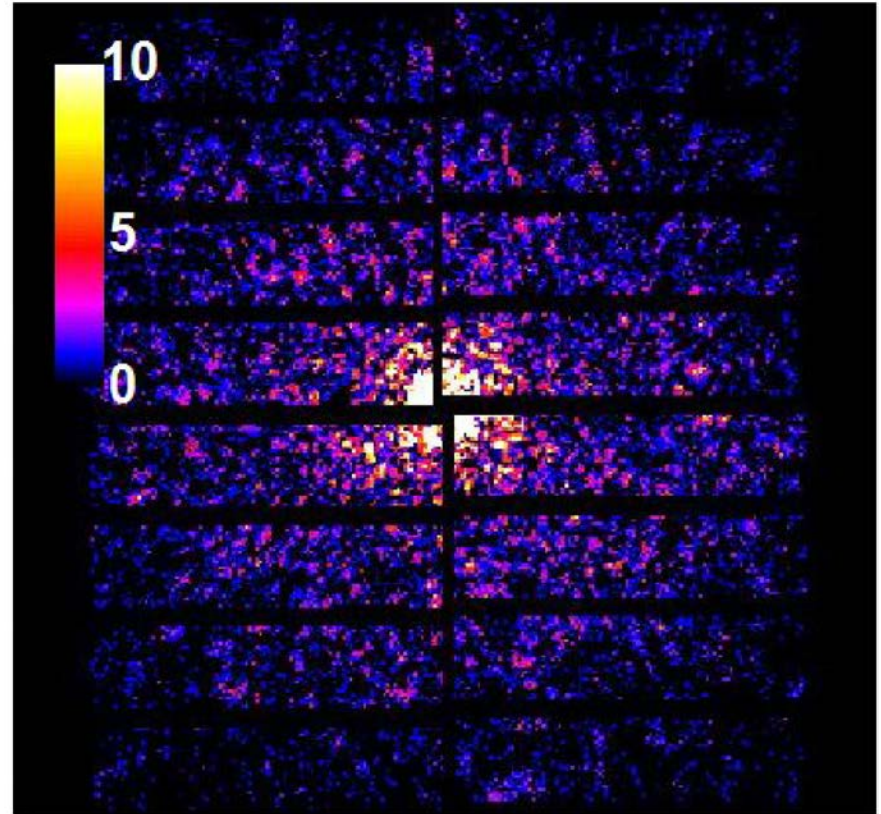
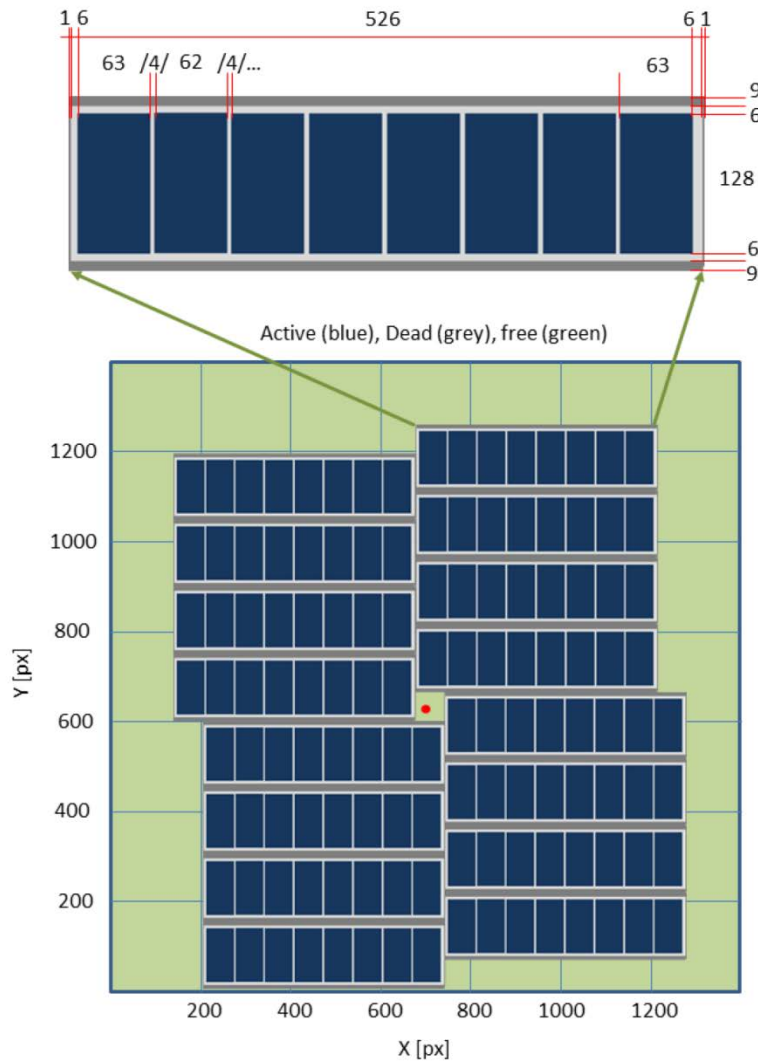
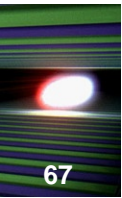
Detector rim \rightarrow 0.39 nm resolution (100 mm from sample).

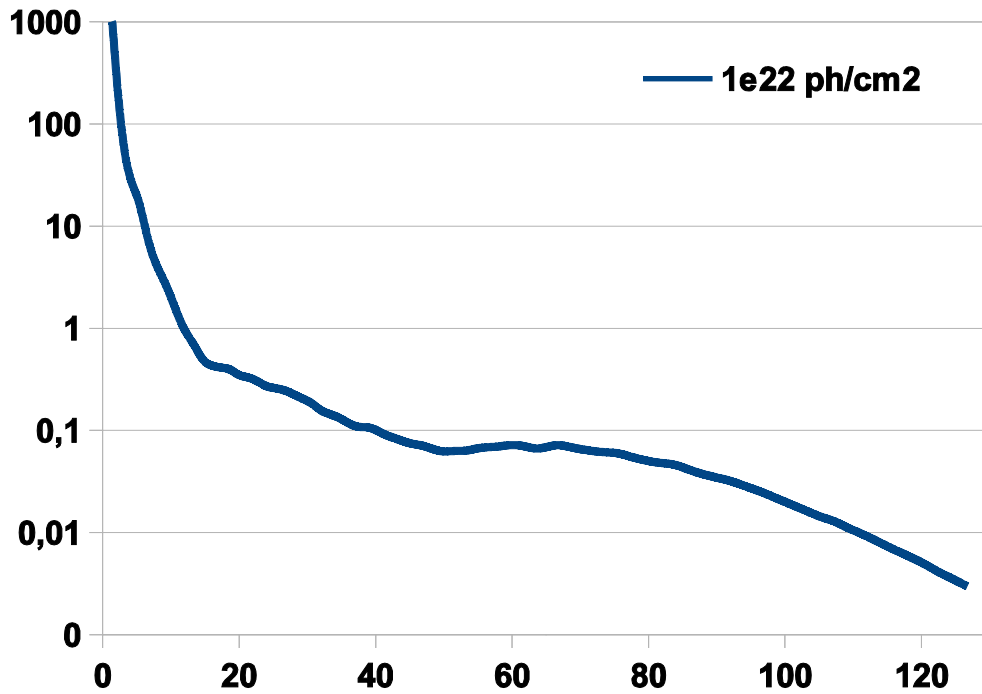
Shannon pixel size \rightarrow 2 mm.

Physical Pixel array dimensions: 200 μ m x 200 μ m \rightarrow 1 Mpix

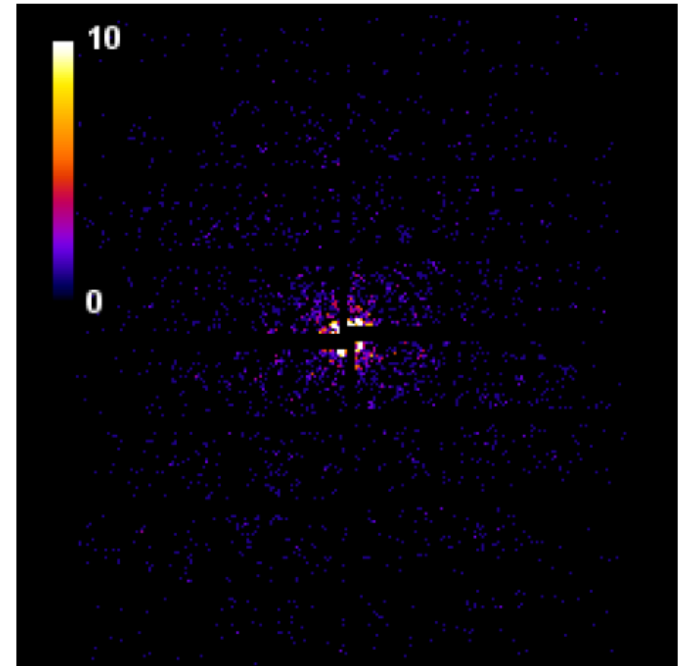
Simulated pixel array: 200x200 (pixel size = 1mm) \rightarrow s=2; b=5

Real detector arrangement

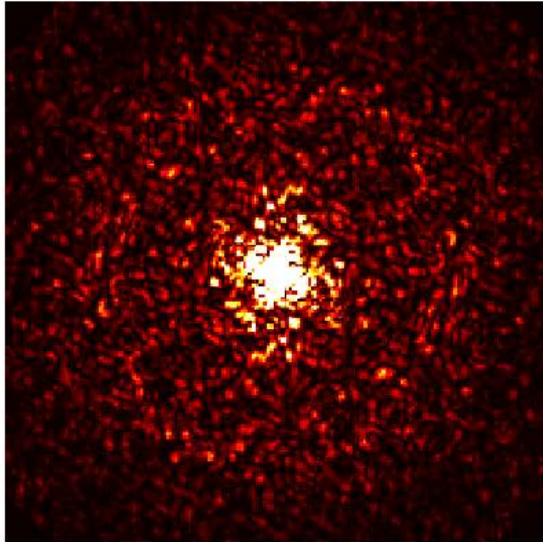




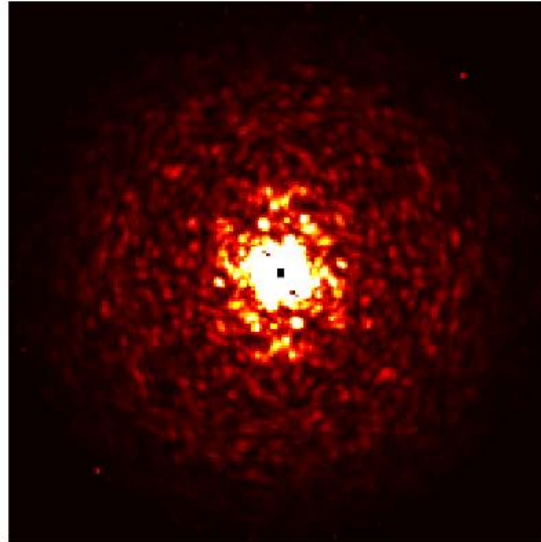
■ Radial average of the photon counts per pixel vs. position along the detector in mm, starting from the center of the detector.



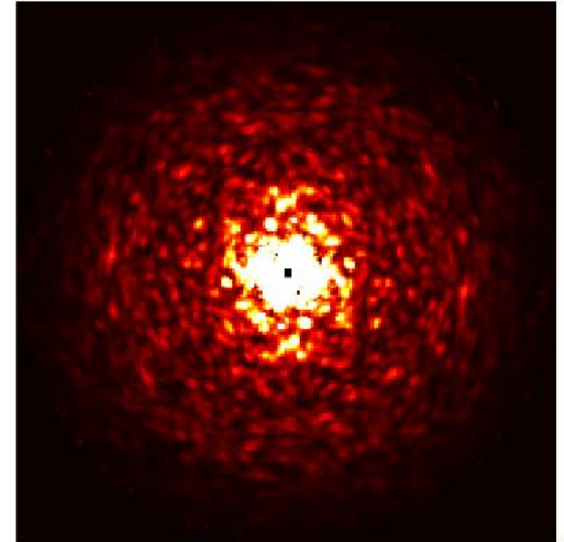
■ Simulated diffraction pattern from the RNA pol II test object as seen by AGIPD detector at a fluence of 10^{22} photons/cm²



(a)



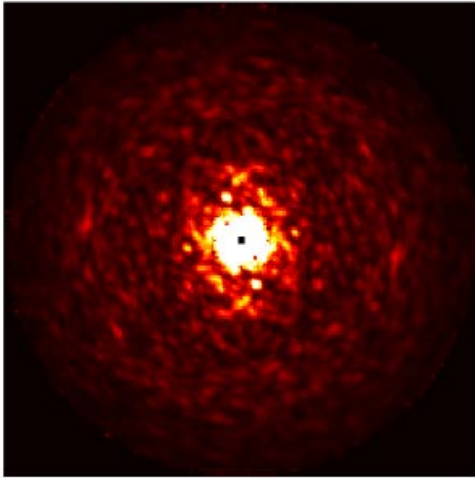
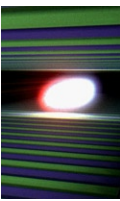
(b)



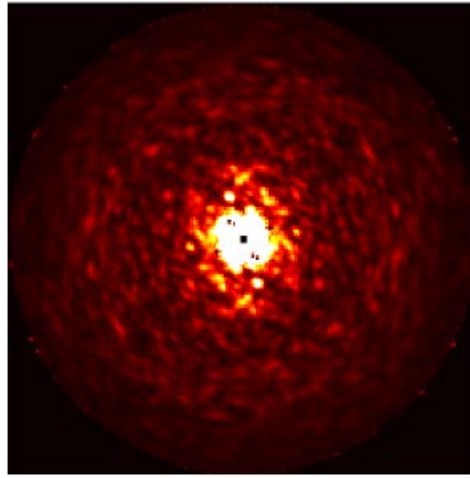
(c)

- (a) Central slice through the ideal intensity distribution of the RNA Pol II distribution.
- (b) Reconstructed intensities using 30,000 patterns with 4000 ph/pattern.
- (c) Same, using 300,000 patterns with 400 ph/pattern.

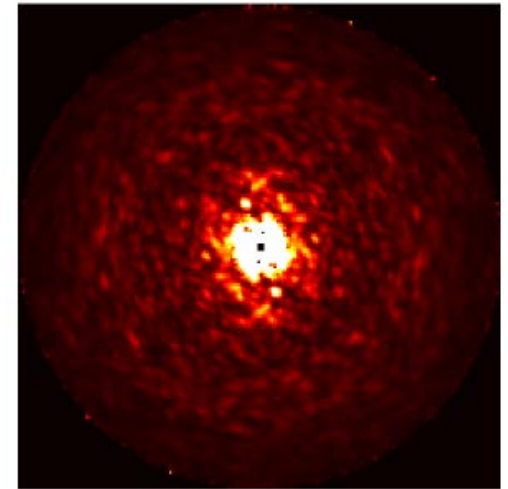
Slices through reconstructed 3D intensities for uniform different background levels. In all cases, there were 150,000 patterns with 800 ph/pattern. At 600 ph/pattern, the reconstruction fails in the manner shown.



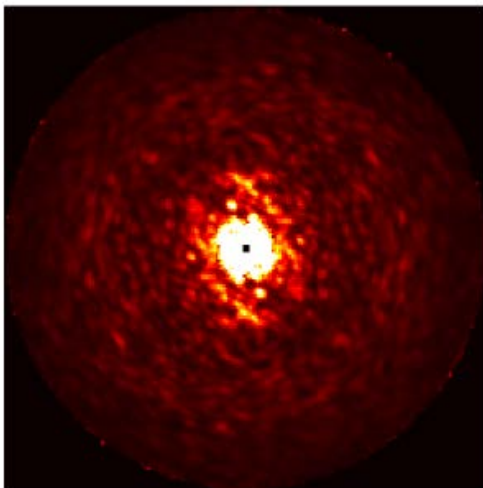
(a) 40 ph/pattern



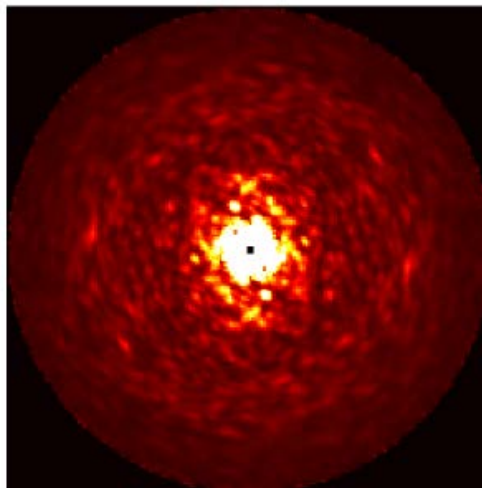
(b) 120 ph/pattern



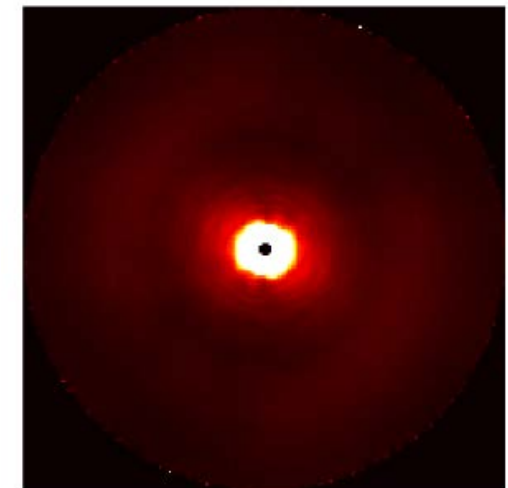
(c) 160 ph/pattern



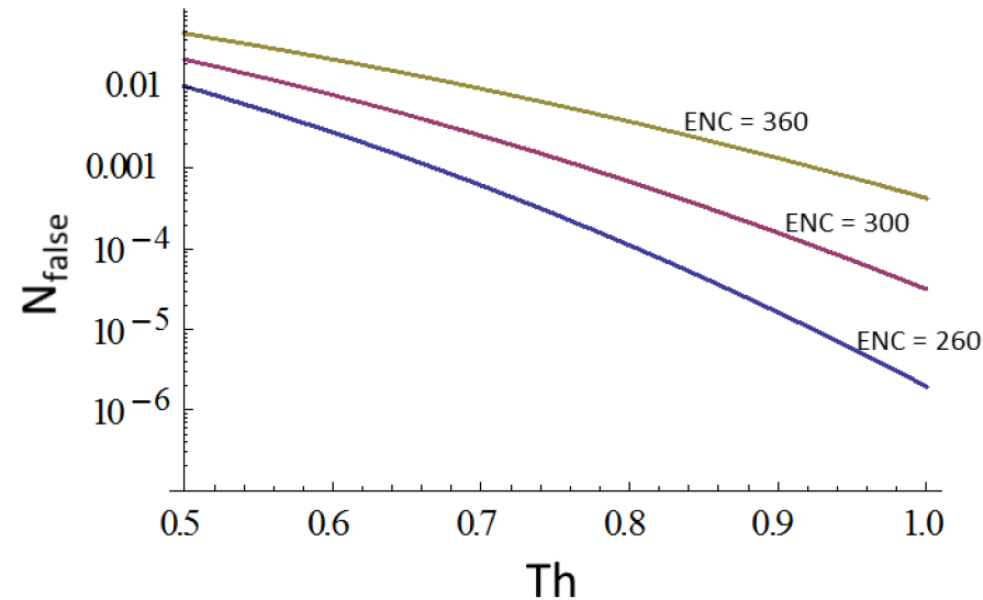
(d) 200 ph/pattern



(e) 400 ph/pattern



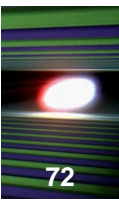
(f) 600 ph/pattern



- Charge amplification in detectors → Noise
- Equivalent noise charge: for AGIPD less than 300 electrons (ENC)
- 1ph@4keV → 1200 electrons
- Assuming Gaussian-distribution random noise in a pix:

$$N_{\text{false}} = \frac{1}{2} \operatorname{erfc} \left(\frac{\text{Th} \cdot N_e}{\sqrt{2} \text{ENC}} \right)$$

Detector noise (intrinsic) negligible



Our results indicate that one can achieve diffraction without destruction with about 0.1 phonons per Shannon pixel per shot at 0.4 nm resolution with 10^{13} photons in a 4 fs pulse at 4 keV photon energy and 300 nm focus, corresponding to fluence 10^{22} ph/cm² .

At signal level of 4000 ph/pattern (corresponding to incident fluence 10^{22} ph/cm²) background level should be < 2000 ph/pattern

At this signal and background level one needs only about 30,000 diffraction patterns to recover full 3D information.

At highest repetition rate manageable by detector at European XFEL (~3000 per second), one is able to accumulate these data within a fraction of an hour, even assuming a relatively low hit probability of about one percent

1. Self-seeded European XFEL offers a unique opportunity for single-biomolecule imaging with high-rate of protein structure determination.
 2. High-repetition rates of self-seeded European XFEL offer a unique opportunity for sub-millivolt inelastic X-ray scattering for nano- and mesoscale science
-



Yaroslav Derbenev, a member of Jlab's Center for Advanced Studies of Accelerators



Anatoly Kondratenko, Director of laser company (Russia)

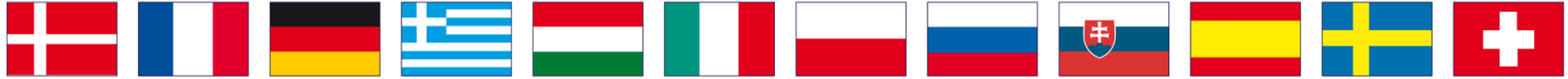
I would like to express my gratitude to Yaroslav Derbenev and Anatoly Kondratenko, who have been teachers and colleagues to me. I feel extremely lucky to have worked for five years alongside such fantastic and dedicated scientists and researchers



BUDKER INSTITUTE OF NUCLEAR PHYSICS

NOVOSIBIRSK, RUSSIA

Place of most powerful XFEL



35 years ago XFELs were not even dreamt of.

Now they are real and this revolution has begun with FLASH, LCLS, SACLA, FERMI...

and will be continued with Swiss FEL, PAL, European XFEL

**Thank you for your attention.
Any questions?**
